Facies (2010) 56:249–278
DOI 10.1007/s10347-009-0204-6

ORIGINAL ARTICLE

Microfacies and depositional setting of the Upper Triassic mid-oceanic atoll-type carbonates of the Sambosan Accretionary Complex (southern Kyushu, Japan)

Jérôme Chablais · Rossana Martini · Elias Samankassou · Tetsuji Onoue · Hiroyoshi Sano

Received: 6 July 2009 / Accepted: 29 October 2009 / Published online: 24 November 2009

Abstract The Upper Triassic shallow-water limestones of the Sambosan Accretionary Complex are reconstructed as a remnant of a mid-oceanic atoll-type build-up upon a seamount in the Panthalassan Ocean. The Sambosan atoll-type carbonates and its pedestal were accreted along with deep-water ribbon-chert and related siliceous rocks to the eastern margin of Asia during the Late Jurassic to Early Cretaceous. Studied limestones crop out in southern Kyushu Island, southwest Japan. Although the prevailing and intense deformation during the accretionary process prevents measurement of sections in stratigraphic successions, and sedimentary structures are poorly preserved, microfacies description and foraminifers analysis allow us to speculate the depositional setting of the Sambosan limestones. Seventeen microfacies are distinguished and several foraminifers of Tethyan affinity are identified. Foraminifers indicate a Late Carnian to Rhaetian age. The Tethyan affinity of the macro- and microfaunas suggests that the Sambosan seamount was located presumably in a low- to middle-latitudinal zone of the southern hemisphere during the Late Triassic.

Keywords Sambosan Accretionary Complex · Seamount · Atoll · Foraminifers · Japan · Panthalassa · Triassic

J. Chablais (✉) · R. Martini · E. Samankassou
Department of Geology and Palaeontology,
University of Geneva, 1205 Geneva, Switzerland
e-mail: Jerome.Chablais@unige.ch

E. Samankassou
Department of Geosciences, University of Fribourg,
1700 Fribourg, Switzerland

E. Samankassou
Faculty of Earth and Life Sciences (FALW),
Free University of Amsterdam, 1081 Amsterdam,
The Netherlands

T. Onoue
Department of Earth and Environmental Sciences,
Kagoshima University, Kagoshima 890-0065, Japan

H. Sano
Department of Earth and Planetary Sciences, Kyushu University,
Fukuoka 812-8581, Japan

Introduction

The overall sedimentology and biostratigraphy of Triassic deposits are well established in the western Tethyan realm and various studies including those dealing with paleogeography and geodynamic models are known: Italy and Sicily (Miconnet et al. 1983; Zaninetti et al. 1984; Senowbari-Daryan et al. 1985; Carcione et al. 2003), Greece (Schäfer and Senowbari-Daryan 1982), Austria (Hohenegger and Piller 1975; Enos and Samankassou 1998; Bernecker et al. 1999), Slovakian and Polish Carpathians (Michalik 1982; Gazdzicki 1983), Oman (Bernecker 1996, 2005; Weidlich et al. 1993; Senowbari-Daryan et al. 1999), Arab Emirates (Maurer et al. 2008; Senowbari-Daryan and Maurer 2008), Indonesia (Al-Shaibani et al. 1983; Villeneuve et al. 1994; Martini et al. 1997, 2004), Philippines (Kiessling and Flügel 2000) and Australia (Kristan-Tollmann and Gramann 1992; Zaninetti et al. 1992). Triassic reefs are particularly well studied (e.g., Kanmera 1964; Flügel 1981; Schäfer and Senowbari-Daryan 1981, 1982; Flügel 1982, 2002; Flügel and Stanley 1984; Stanley and Gonzalez-Leon 1997; Senowbari-Daryan et al. 1999; Bernecker et al. 1999; Kiessling et al.

1999). By contrast, Triassic sequences that were originated in the Panthalassan Ocean are poorly documented. Furthermore, only a few comparative studies have been conducted between Panthalassan and Tethyan provinces (Kristan-Tollmann 1986, 1988, 1991; Stanley 1994). Thus, the understanding of the Late Triassic Panthalassan paleoenvironment and its comparison with that of the Tethyan realm is of great importance for the global paleogeographic reconstructions. The study of the Sambosan Accretionary Complex (AC) allow us to resolve a part of these reconstructions. Indeed, the occurrence of extensive limestone and basaltic rocks, and their stratigraphic relation suggest that most of the Sambosan rocks were derived from a submarine Panthalassan seamount province. Matsuoka (1992) deduced that the Sambosan AC results from collision-accretion of a Triassic seamount province that reached a convergent margin during the Late Jurassic to Early Cretaceous.

The present work aims to: (1) define and interpret the microfacies of the Sambosan AC Upper Triassic limestones to better understand the Late Triassic mid-oceanic sedimentation in the Panthalassa Ocean, and (2) show a speculative depositional profile of the Sambosan atoll-type facies. Much attention is paid to reefs with an emphasis upon their high sensitivity to changes in environmental factors. Specifically, the study of foraminifers offers new insight into the depositional environment.

Geological setting

Japanese Pre-Cretaceous basement rocks represent an accretionary complex that assembled as a result of accretion and collision of several micro-continents, island arcs, ridges, seamounts, and deep-oceanic sediments (Kobayashi 2003). In Late Palaeozoic-Early Mesozoic time, these oceanic rocks or terranes were located in the ancient oceanic plates of the Panthalassa within tropical to subtropical latitudinal zones. These rocks were accreted to the eastern margin of the ancient Asian continent by subduction of oceanic plates (Taira et al. 1989; Isozaki 1997; Wakita and Metcalfe 2005). These ancient accretionary complexes forming Japanese Islands can be differentiated into three major groups according to their age of accretion: Pre-Jurassic, Jurassic to Early Cretaceous, and Cretaceous to Mid-Cenozoic, respectively (Ichikawa 1990). With regard to this study, the Sambosan AC comprises an unmetamorphosed Late Jurassic to Early Cretaceous subduction-generated accretionary complex in southwestern Japan (Onoue et al. 2004).

The Sambosan AC can be traced in a narrow belt (Fig. 1), approximately 5 km wide at the maximum, and extending for more than 1,000 km from the Ryukyu Islands (Motobu Peninsula and Cape Hedo, Okinawa Island) to the Kanto Mountains, central Japan (Matsuoka and Yao 1990; Matsuoka 1992). The southernmost exposure area is on

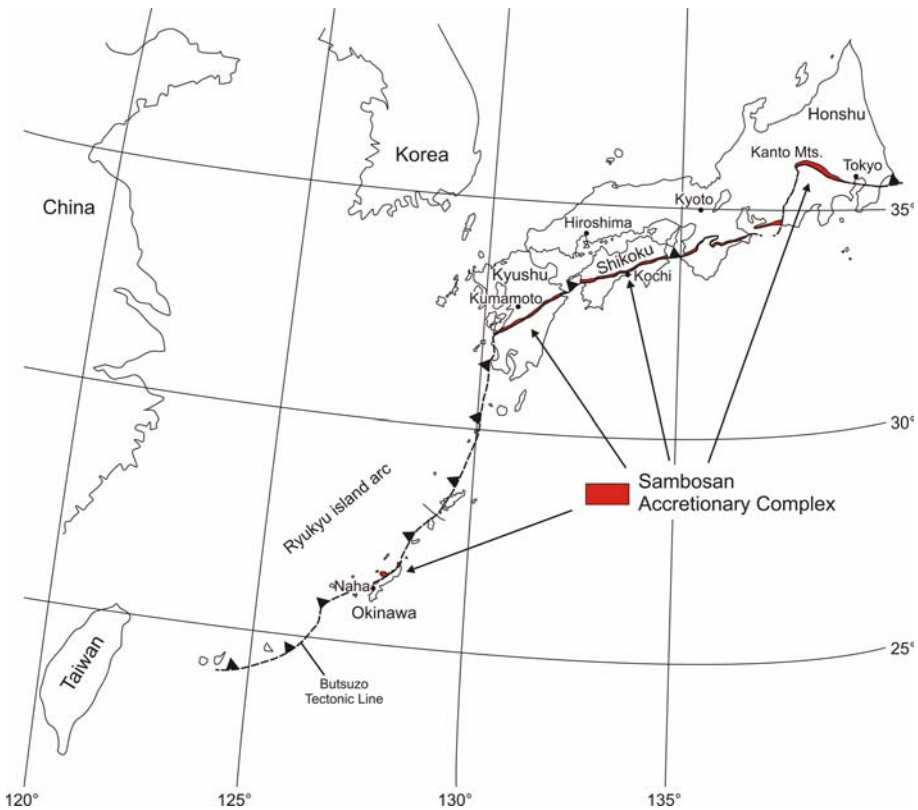

Fig. 1 Distribution of the Sambosan Accretionary Complex (*red*), exposed in a narrow belt extending from the Ryukyu Islands to the Kanto Mountains, central Japan

Okinawa Island (Fujita 1989; Takami et al. 1999) and extends as far as eastern Russia (Kojima 1989; Faure and Natal'in 1992). The Sambosan AC is tectonically separated from the Jurassic Chichibu AC to the north and from the Lower Cretaceous-Palaeogene Shimanto AC to the south. The contact to the Shimanto AC is referred to as the Butsuzo Tectonic Line. The Chichibu, Sambosan, and Shimanto accretionary complexes together form a north-dipping and southeast-verging imbricate stack with a southward-younging age-polarity (Onoue and Sano 2007).

Major components of the Sambosan AC (Fig. 2) are Middle Triassic to lower Upper Jurassic siliceous ribbon cherts and related siliceous rocks, middle Upper Triassic basaltic rocks, Upper Triassic shallow- and deep-water limestones, and lower Middle to Upper Jurassic siliceous mudstone/sandstone (Kanmera 1969; Matsuoka and Yao 1990; Onoue and Sano 2007). Of these components, Upper Triassic limestones best characterize the Sambosan AC.

They commonly occur associated with basaltic volcaniclastic rocks and include several microfacies types and shallow-marine fossils, including corals, sponges, bivalves, crinoids, foraminifers, and calcareous algae. Historically, the shallow-water limestones were first studied by Kobayashi (1931), who reported Late Triassic bivalves. Kanmera (1964, 1969) and Kanmera and Furukawa (1964) first described lithofacies, including reefal and deep-water facies, and coral faunas. Tamura (1972, 1981, 1983) reported on the distribution of megalodonts and other bivalves. Kristan-Tollmann (1991) analyzed and illustrated Norian-Rhaetian foraminifers in Kyushu and eastern Honshu. She highlighted the resemblance of these regions to the Austrian Alps (Dachstein platform). Recent studies of these Upper Triassic shallow-water limestones were made by Onoue and Tanaka (2002, 2005), Onoue and Sano (2007) and Onoue and Stanley (2008).

Concerning the other oceanic rocks, the pelagic deep-water limestone (the siliceous micrite of Onoue and Sano 2007) occurs intercalated within ribbon-bedded radiolarian cherts and ranges in age from Late Carnian to Early Norian. It contains radiolarians and numerous filaments of thin-shelled bivalves.

The basaltic rocks are interpreted as oceanic island basalt (OIB) based on geochemistry (Ogawa and Taniguchi 1989; Onoue et al. 2004). They consist of dark reddish or greenish pillow lavas, pillow breccia, and volcaniclastic rocks (Onoue et al. 2004). Based on the occurrence of the conodont *Metapolygnathus nodosus* extracted from the micritic interpillow limestone, Onoue and Sano (2007) estimated the eruption of the Sambosan basalts to have occurred in the Late Carnian, and therefore also dating the main basaltic rocks as Late Carnian. The presence of this micritic interpillow limestone containing skeletal debris indicates that the Sambosan basalts were formed above the carbonate compensation depth

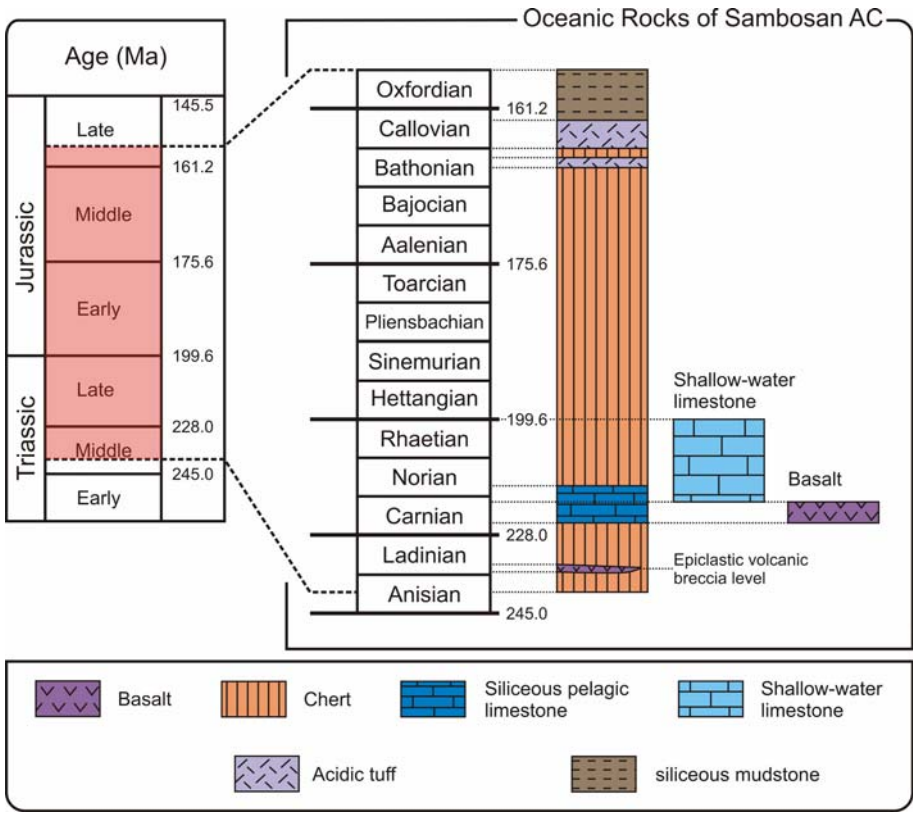

Fig. 2 Stratigraphic summary of Triassic to Jurassic Sambosan oceanic rocks, modified after Onoue and Sano (2007). Oceanic rocks can be subdivided into three rock successions: (1) the siliceous rocks containing ribbon chert, siliceous pelagic limestone, acidic tuff, and siliceous mudstone units; (2) the shallow water sequence during the Late Triassic; and (3) the main basaltic stage related to seamount eruption, dated Late Carnian using conodonts from micritic interpillow limestones. Rare intermittent beds of epiclastic volcanic breccia also occur during Ladinian

(CCD) and at a shallow-water depth (Onoue and Sano 2007). A small intermittent bed of epiclastic volcanic breccia (pebble- to cobble-sized basalt clasts) occurs intercalated between the chert successions during the Early Ladinian, but is not related to the main eruption stage during the Late Carnian.

Cherts are usually ribbon-bedded and locally massive, commonly white to brownish white, and composed dominantly of microcrystalline to cryptocrystalline quartz. They contain abundant densely packed radiolarians, used for datation, and a few siliceous sponge spicules. The chert succession belongs to an important siliceous rock succession stratigraphically subdivided into a lower ribbon chert, siliceous pelagic limestone, upper ribbon chert, uppermost acidic tuff and mudstone units, as well as rare intermittent beds of epiclastic volcanic breccia (Fig. 2).

The overall biostratigraphy of the Sambosan AC is based on conodonts (Koike 1981; Onoue and Tanaka 2005), radiolarians (Yao 1990; Nishizono 1996; Onoue et al. 2004), corals (Kanmera 1964), bivalves (Tamura 1972, 1981, 1983; Onoue and Tanaka 2005) and foraminifers (Kristan-Tollmann 1991; Chablais et al. 2007, 2008). Currently, the Sambosan limestones are assumed to be Carnian to Norian in age (Kanmera 1964; Koike 1981; Kristan-Tollmann 1991; Onoue and Tanaka 2005). Cherts are though to be Middle Triassic to Late Jurassic and terrigenous mudstones to be Late Jurassic to Early Cretaceous in age (Nishizono 1996; Onoue et al. 2004). Onoue and Sano (2007) give a precise overview of the Sambosan lithostratigraphy.

Studied areas and field characters

The studied area is located in Kyushu Island, southwest Japan. The selection of the localities relied on the geological map of Onoue and Tanaka (2002) and Onoue et al. (2004). Sampling was limited to outcrops along rivers and road cuts due to the overall intensive vegetation cover. Two main areas were selected for sampling. The first, Kumagawa, is located along the Kumagawa (latitude: 32°16′43.75″N and longitude: 130°36′32.72″E) and Nakazono (latitude: 32°17′15.72″N and longitude: 130°38′11.51″E) rivers, southeast of Yatsushiro City. The second corresponds to the Itsuki area north of Hitoyoshi City in the Motoidani Gully (latitude: 32°23′18.19″N and longitude: 130°47′20.36″E) and Hachibaru Mountains (latitude: 32°24′19.72″N and longitude: 130°51′0.46″E) (Fig. 3).

Rocks at 19 outcrops have been sampled. Lithologies were mapped in the field and, where necessary, the existing geological map was modified. Route-maps were also added to the map for a better localization of the collected samples (Fig. 4).

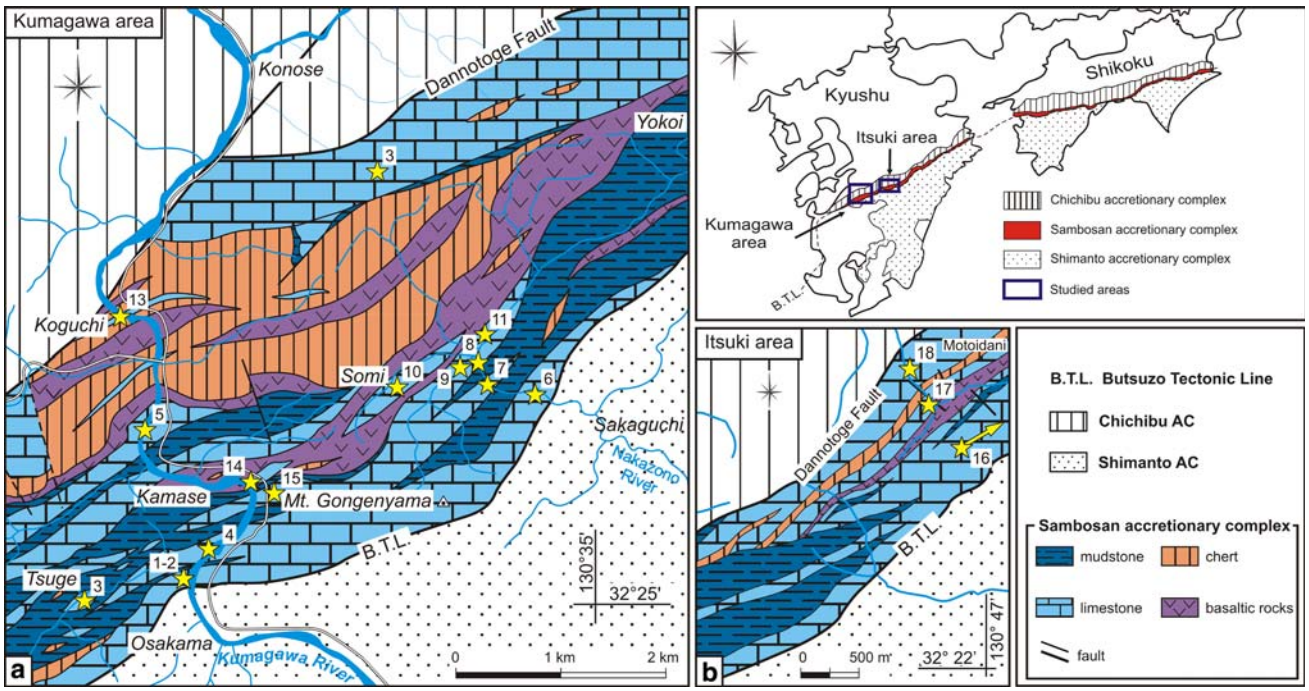

Fig. 3 Geological maps of **a** Kumagawa and **b** Itsuki areas. Studied outcrops are indicated by *yellow stars*. Modified from Onoue and Tanaka (2002) and Onoue et al. (2004)

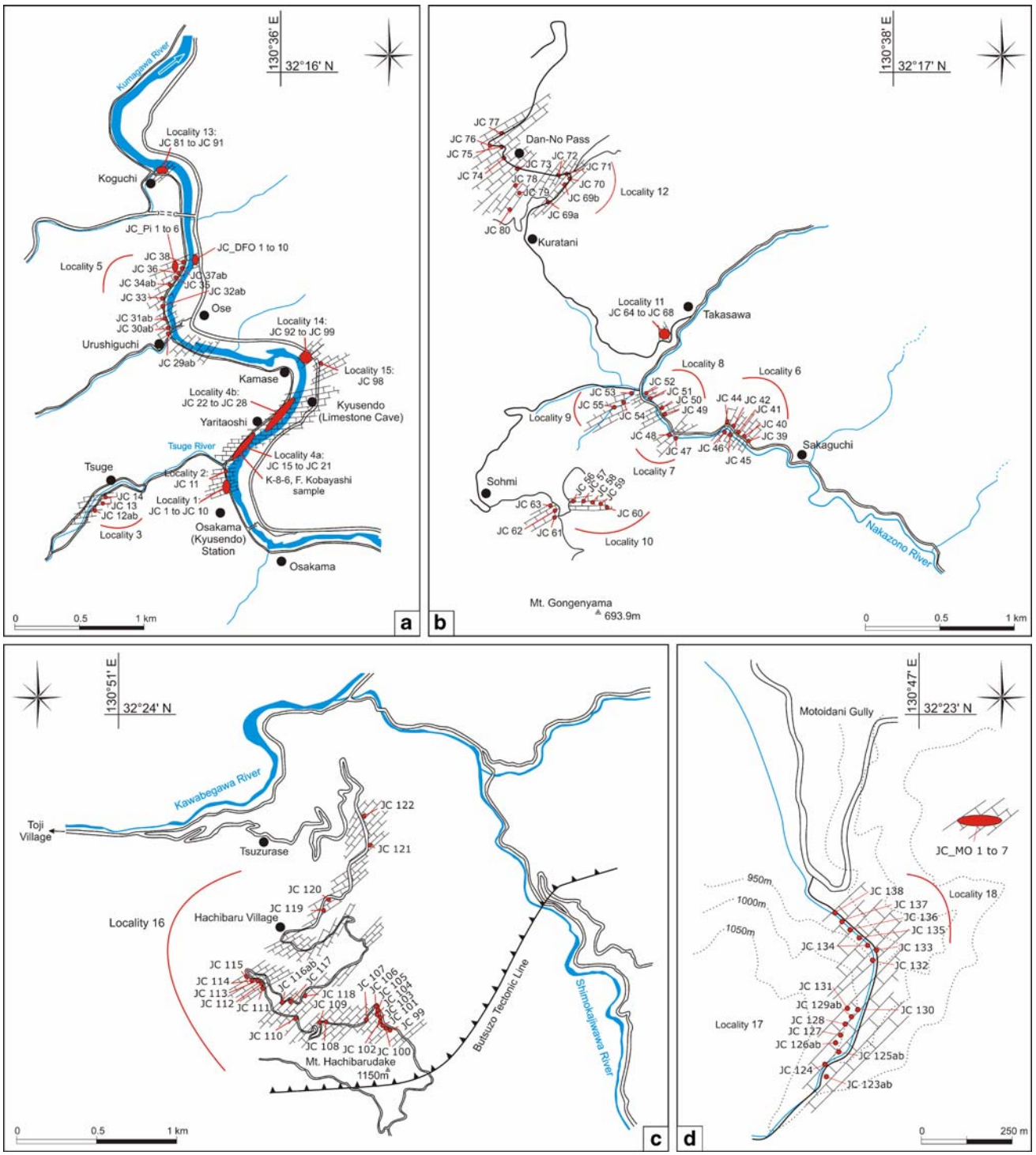

Fig. 4 Route-maps along **a** Kumagawa River, **b** Nakazono River, **c** near Mt. Hachibarudake, and **d** in the Motoidani Gully with samples (with *JC* for prefix) and outcrop locations (Localities *1* to *18*). Locality *19*, situated between Kumagawa and Itsuki areas, is out of the mapped areas

Limestone preservation is poor due to the intense shearing during the accretion process and tectonic faults. Tectonic produced important macro- and microfracturing and an extensive recrystallization.

Furthermore, the primary stratigraphy of the Upper Triassic limestone of the Sambosan AC, as well as basaltic and chert rocks, have been largely disrupted to form various-sized and isolated blocks, set in a volcaniclastic matrix, and interpreted as tectonic debris avalanche and debris flow deposits resulting from submarine landslides of a seamount in a mid-oceanic setting during the Middle to Late Jurassic (Onoue et al. 2004; Onoue and Sano 2007; Onoue and

Stanley 2008). This major dismantling of seamounts before the accretion produced a first mélange of shallow- and deep-water limestone, basalt and chert units, all set in this volcaniclastic matrix. This first mélange was dismantled a second time during accretion and incorporated into terrigenous sediments including siliceous mudstone and sandstone.

In the field, the Upper Triassic limestone mainly crops out as three modes of occurrence (Fig. 5):

1. Type 1—Massive limestone blocks, partly brecciated, several tens of meters to a few meters in size. Each huge block generally shows extensive fracturing and recrystallization.
2. Type 2—Clast-supported limestone breccias with limestone clasts of different sizes. Locally, clasts of basalt and cherts occur.
3. Type 3—Limestone pebbles, centimeters in size, associated with chert and basaltic pebbles within a volcaniclastic matrix.

Types 1 and 2 are currently comprised within a volcaniclastic matrix or within a mudstone matrix. The matrix of volcaniclastic rocks is sand to mud-sized containing angular basaltic lava debris with a minor amount of vesicular glass shards (Onoue and Stanley 2008). These volcaniclastic sediments have numerous possible scenarios to be generated, but their origin remains uncertain. We observed that during the accretion, massive limestone blocks (type 1), which were comprised within a mudstone matrix (second mélange matrix), are much more recrystallized than those that were preserved within a volcaniclastic matrix (first mélange matrix).

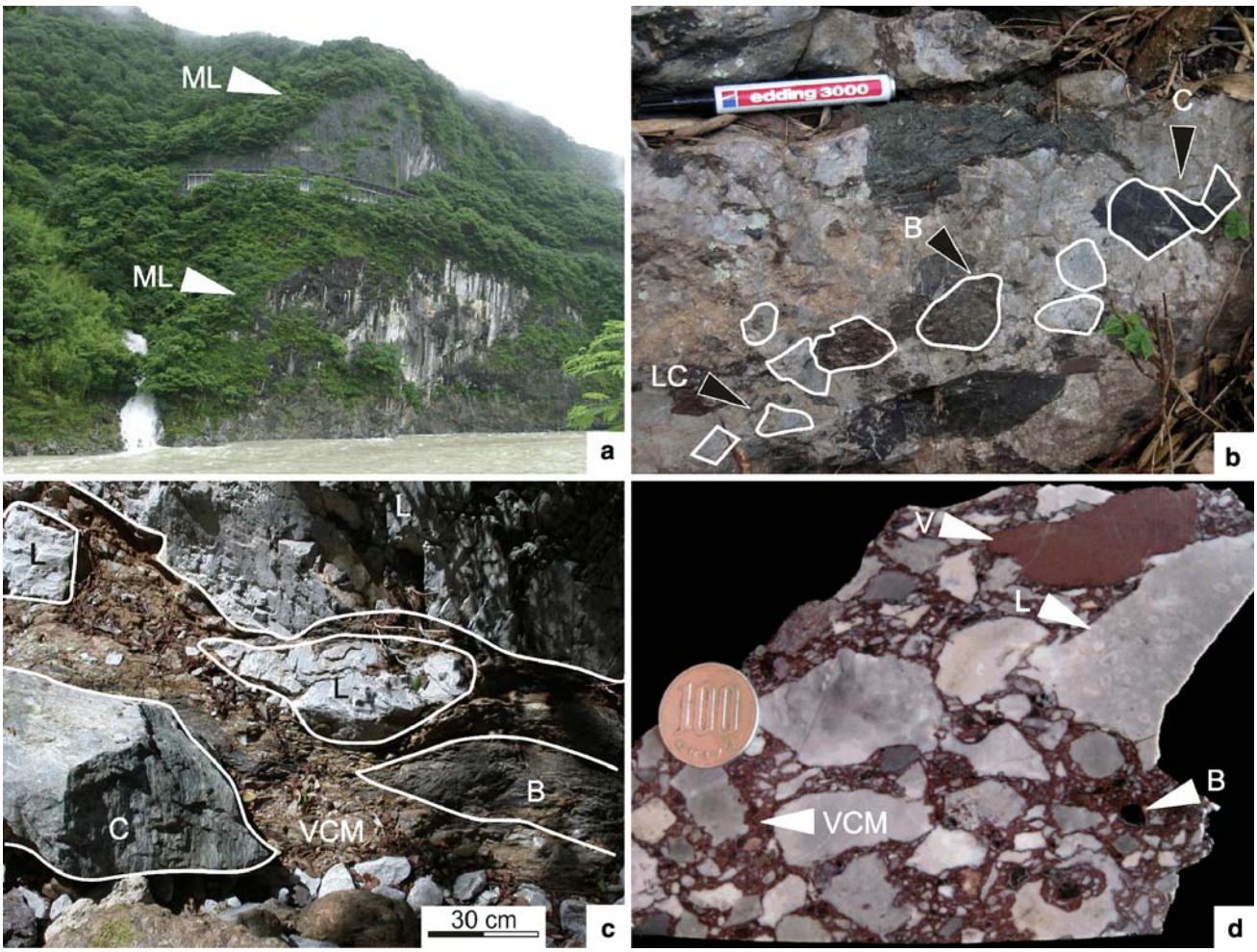

Fig. 5 Outcrop views and polished slab of limestone and volcaniclastic rocks-mixed facies: **a** Type 1: massive limestone blocks (*ML*); locality 4. **b** Type 2: limestone breccia with limestone (*L*), basalt (*B*) and chert (*C*) clasts; locality 5. **c** Type 3: debris flow deposit including large-sized limestone (*L*), basalt (*B*) and chert blocks (*C*) within a volcaniclastic matrix (*VCM*); locality 9. **d** Type 3: debris flow deposit with pebbles-sized clasts of limestone (*L*), basalt (*B*) and volcaniclastic (*V*) within a volcaniclastic matrix (*VCM*). Most of the limestone clasts have a shallow-water affinity; locality 5

In addition, three subordinate types of limestone deposits, in which brecciation and/or reworking are absent, also occur: pelagic limestones intercalated between bedded cherts rich in filaments and radiolarians indicating Late Carnian to Early Norian age (Onoue and Sano 2007); pelagic micritic interpillow limestones within the basaltic outcrops containing conodonts that give a Late Carnian age for the eruption of the basaltic lavas; and rare thin-bedded dark limestone's resting upon and alternating with the basaltic volcaniclastic rocks (Onoue and Tanaka 2005).

The next chapters will be based on the results of the microfacies analysis of approximately 300 thin-sections. Samples were systematically collected in the limestone types 1 to 3, as well as some in the pelagic and bedded ones. The relative abundance of components in thin-sections has been estimated using both point-counting analysis and the comparison charts of Flügel (2004). Furthermore, the data offer more insight into micropaleontology and biostratigraphy. These analyses enable to characterize the Sambosan AC shallow- and deep-water limestones and to speculate their depositional setting using facies models for time-equivalent and modern platform carbonates.

Facies description

We differentiated 17 microfacies types using the nomenclature of Dunham (1962). Particular attention was paid to benthic foraminifers. Facies description and interpretation are summarized in Table 1. It is important to note that except for MF 16 and MF 17, all the microfacies are of the shallow-water limestone type.

MF 1: Limestone microbreccia (Fig. 6a–b)

Dark grey to light grey massive limestone blocks, limestone breccia or limestone pebbles (types 1, 2 and 3). Clasts are subangular to angular, locally completely disorganized, and mainly supported by a voclaniclastic matrix. Their size ranges from millimetric to centimetric scales. Clasts mainly correspond to shallow-water limestones, dominantly peloidal or oolitic grainstone, rich in skeletal debris including algae, calcimicrobes, and echinoderms. Subordinate clasts are basalt and deep-water limestones, including radiolarian lime-mudstone and thin-shelled bivalve mudstone. A grading in grain size is locally observed.

MF 2: Crinoidal-algal packstone-grainstone (Figs. 6c, 10e-f)

Light grey limestone breccia or limestone pebbles (types 2 and 3). This packstone-grainstone is composed of abundant fragments of crinoids and echinoids (15–25%), and algae (20%). Algal debris, of which a few have internal structure preserved, are subrounded to subangular. Subordinate components are peloids, micritic particles, calcareous sponges, rare corals, debris of molluscan shells, rare gastropods, and a few benthic foraminifers such as *Duostomina* sp., *Variostoma* sp., and *Diplotremina* sp. The matrix is sparite, locally with relics of micrite. Drusy mosaic cement is common.

MF 3: Sponge-coral-algal boundstone (Figs. 6d–e, 7a–c, 10g–m, 11a–e)

Massive grey limestone blocks, limestone breccia or limestone pebbles (types 1, 2 and 3). Blocks or pebbles are composed of boundstone facies, where the reefal components are calcareous sponges (sphinctozoan, inozoan, and spongiomorphids), scleractinian corals, algal-microbial crusts, solenoporacean red algae, *Parachaetetes* sp. and microbial laminated stromatolites or spongiostromata crusts. Corals have dendroid and branching growth forms. Sponges are spheriform and digitate. Subordinate components include debris of algae (rare dasycladacean green algae), the incertae sedis *Tubiphytes*, microproblematica such as *Microtubus communis*, bryozoans, fragments of bivalve shells, crinoids and echinoids, smaller benthic foraminifers, ostracods, peloids, and rare ooids and calcimicrobes. Skeletal debris are overall poorly sorted and set in a micritic or sparitic matrix. Fragments of bioclasts are well rounded. The benthic foraminifer assemblage includes *Agathammina austroalpina*, *Glomospira* sp., *Glomospirella* sp., *Hoyenella inconstans*, *Endotriada thyrrenica*, *Galeanella panticae*, "*Trochammina*" sp., *Ophthalmidium* spp., *Hirsutospirella* cf. *pilosa* and some attached foraminifers such as *Planiinvoluta* sp.. Sponges and corals are commonly recrystallized by sparry calcite, but preservation of the internal structures is necessary for determination at the genera level. However, Kanmera (1964) determined many corals including three species of *Montlivaltia* sp., *Thecosmilia* sp., and *Pyrocyclolites* sp., two species of *Thamnasteria* sp., and one of *Oppelsimilia* sp., *Elysatrea* sp. and *Conophyllia* sp. Onoue and Stanley (2008) identified the following genera of solitary corals in locality 14: *Cuifia ominensis* and *Distichophyllia* sp., and colonial corals including *Retiophyllia eguchi* and *Retiophyllia* sp. The spongiomorphids occur generally as small fragments. Laminations consisting of parallel micritic peloidal layers alternating with coarse-sparry calcite cement layers are present. The peloidal layers contain ostracods, and unidentified bioclasts filled by sparite. The spongiomorphids are generally found as lithoclasts in this reefal boundstone. The crusts vary from a few millimeters to few centimeters in thickness. Radiaxial fibrous cement grew

Table 1 Summary of microfacies type characterizing the Upper Triassic atoll-type shallow- and deep-water limestones of Sambosan AC, southern Kyushu Island, Japan

Facies type	Localities	Biotic components	Associated benthic foraminifers	Samples	Facies interpretation
Limestone microbreccia (MF 1)	Kumagawa (c) and Itsuki areas (c)	Sand-size grains or clasts of shallow-water limestone or pelagic deeper limestone of several kinds	–	Dark grey to light grey massive limestone blocks, limestone breccia, or limestone pebbles (types 1, 2, and 3) Localities 1, 5, 6, 7, 13, 18, and 19	Slope
Crinoidal-algal packstone-grainstone (MF 2)	Kumagawa (c) and Itsuki areas (r)	*Major*: fragments of crinoids, echinoids and algae. *Subordinate*: peloids, micritic particles, debris of molluscan shells, rare gastropods, and a few benthic foraminifers	*Duostomina* sp., *Variostoma* sp., and *Diplotremina* sp. [Upper Triassic]	Dark grey to light grey limestone breccia or limestone pebbles (types 2 and 3) Localities 1, 5, 7, 13, 18, and 19	Fore-reef
Sponge-coral-algal boundstone (MF 3)	Kumagawa (c) and Itsuki areas (r)	*Major*: calcareous sponges (sphinctozoan and inozoan), spongiomorphids), scleractinian corals, algal-microbial crusts, solenoporacean red algae, and microbial laminated stromatolites or spongiostromata crusts *Subordinate*: debris of algae, rare dasycladacean green algae, the *incertae sedis Tubiphytes* sp., microproblematica such as *Microtubus* sp., bryozoans, fragments of bivalve shells, crinoids and echinoids, smaller benthic foraminifers, ostracods, peloids and rare ooids and calcimicrobes	*Agathammina austroalpina, Glomospira* sp., *Glomospirella* sp., *Hoyenella inconstans, Endotriada thyrrenica, Galeanella panticae,* "*Trochammina*" sp., *Ophthalmidium* sp., *Hirsutospirella* cf. *pilosa* and *Planiinvoluta* sp. [Late Carnian to Norian-Rhaetian]	Massive grey limestone blocks, limestone breccia or limestone pebbles (types 1, 2 and 3) Localities 5, 8, 10, 13, 14, 15, and 16	Reef (reef margin or patch-reef)
Peloidal-aggregate-bioclastic packstone-grainstone (MF 4)	Kumagawa (c) and Itsuki areas (r)	*Major*: peloids, aggregate grains, algal debris and coated grains *Subordinate*: porostromate oncoids, tubular algae, bivalve shells, gastropods, echinoid spines, crinoid debris, extraclasts, rare ooids, and benthic foraminifers	*Duostomina* sp., *Variostoma* sp., *Diplotremina* sp, aulotortids, and rare *Glomospira* sp., *Glomospirella* sp., *Textularia* sp., *Gsolbergella spiroloculiformis*, *Ophthalmidium* sp., *Endotriada* sp. and *Endoteba* sp. [Upper Triassic]	Grey to light grey limestone breccia or limestone pebbles (types 2 and 3) Localities 1, 5, 8, 9, 10, and 16	Back-reef—lagoon

Table 1 continued

Facies type	Localities	Biotic components	Associated benthic foraminifers	Samples	Facies interpretation
Calcimicrobial grainstone (MF 5)	Kumagawa (c) and Itsuki areas (r)	*Major*: calcimicrobes *Cayeuxia* and *Garwoodia* *Subordinate*: peloids, aggregate grains, echinoderm fragments, and rare benthic foraminifers	Duostominids [Upper Triassic]	Grey to light gray limestone breccia or limestone pebbles (types 2 and 3) Locality 5	Back-reef—lagoon
Mudstone (MF 6)	Kumagawa (c) and Itsuki areas (c)	*Major*: homogenous micrite *Subordinate*: ostracods, peloids, and rare skeletal grains	–	Light to dark grey massive limestone blocks or limestone breccia (types 1 and 2) Localities 4, 16, 17, 18, and 19	Lagoon
Endotebid mudstone (MF 7)	Itsuki area (r)	*Major*: *Endoteba controversa* and *Endotriada thyrrenica* *Subordinate*: benthic foraminifers, small gastropods, ostracods, thin bivalve shells and uncommon echinoderm fragments	*Endoteba* ex. gr. *controversa*, *Endotriada thyrrenica*, *Aulotortus* sp., Textularia sp., *Ammodiscus* sp., *Triadodiscus eomesozoicus*, *Ophthalmidium* sp., *Paraophthalmidium* sp., *Duostomina* sp., *Agathammina austroalpina*, *Gsolbergella spiroloculiformis* and *Fondicularia woodwardi*. [Late Carnian to Norian (-Rhaetian?)]	Thin-bedded dark limestones Locality 17	Lagoon
Megalodont floatstone (MF 8)	Kumagawa (c) and Itsuki areas (a)	*Major*: large megalodont shells: *Triadomegalodon* sp. and *Dicerocardium kuwagataforme* *Subordinate*: debris of bivalves, gastropods, benthic foraminifers, echinoids, crinoids, ostracods, peloids, microcoprolites and indeterminable sparite-filled bioclasts	Aulotortids and nodosariids [Upper Triassic]	Grey to dark grey massive limestone blocks (type 1) Localities 4 and 17	Lagoon

Table 1 continued

Facies type	Localities	Biotic components	Associated benthic foraminifers	Samples	Facies interpretation
Echinoderm-bioclastic wackestone-packstone (MF 9)	Kumagawa (c) and Itsuki areas (c)	*Major*: echinoid spines and crinoid debris *Subordinate*: skeletal coarse-grains, gastropods, aulotortid foraminifers, large bivalve shells fragments such as megalodonts, holothurian sclerites, sponge spicules, rare ostracods and indeterminable sparite-filled bioclasts.	Aulotortids [Upper Triassic]	Dark grey to grey massive limestone blocks or limestone breccia (types 1 and 2) Localities 2, 6, 10 and 16	Lagoon
Aulotortid packstone (MF 10)	Kumagawa (a) and Itsuki areas (a)	*Major*: aulotortid foraminifers *Subordinate*: bivalve shell fragments (essentially megalodonts), gastropods, ostracods, echinod and crinoid fragments, serpulids, other benthic foraminifers, rare peloids, and indeterminable sparite-filled bioclasts	*Aulotortus* ex. gr. *sinuosus*, *A. communis*, *A. tenuis*, *A. gaschei*, *Auloconus permodiscoides*, *Triasina hantkeni,* nodosariids *(Frondicularia* sp.) *Agathammina austroalpina* [Late Carnian to Norian-Rhaetian]	Grey to dark grey massive limestone blocks or limestone breccia (types 1 and 2) Localities 4, 16 and 17	Lagoon
Coprolite-bioclastic wackestone-packstone (MF 11)	Kumagawa (r) and Itsuki areas (c)	*Major*: crustacean microcoprolites and debris of bivalve shells *Subordinate*: benthic foraminifers, peloids, gastropods, ostracods, echinoderm fragments and indeterminable sparite-filled bioclasts	Aulotortids and nodosariids Microcoprolites: *Payandea japanica*, *Favreina tosaensis*, and *Favreina*? sp.-*Parafavreina*? sp. [Upper Triassic]	Dark grey massive limestone blocks or limestone breccia (types 1 and 2) Localities 3, 16 and 17	Lagoon
Molluscan-burrowed wackestone (MF 12)	Itsuki area (c)	*Major*: bivalve shells and large peloids *Subordinate*: gastropods, ostracods, smaller benthic foraminifers and indeterminable sparite-filled bioclasts	*Endotriada* sp., *Endoteba* sp., *Agathammina austroalpina* and few aulotortids and nodosariids [Late Carnian-Norian to Rhaetian]	Dark to grey massive limestone blocks or limestone breccia (types 1 and 2) Locality 17	Lagoon
Peloidal-bioclastic packstone-grainstone (MF 13)	Kumagawa (a) and Itsuki areas (c)	*Major*: peloids and skeletal debris *Subordinate*: algal fragments, bivalves, gastropods, crinoids and echinoids, ostracods, few ooids, rare benthic foraminifers and indeterminable sparite-filled bioclasts	Aulotortids, nodosariids and duostominids [Upper Triassic]	Dark grey to grey massive limestone blocks or limestone breccia (type 1 and 2) Localities 11, 12, 16 and 19	Lagoon

Table 1 continued

Facies type	Localities	Biotic components	Associated benthic foraminifers	Samples	Facies interpretation
Foraminiferal grainstone (MF 14)	Kumagawa area (r)	*Major*: benthic foraminifers *Subordinate*: coated grains, ooids, peloids, bivalves shells fragments, gastropods, algal debris, crinoids, echinoids and rare debris of porostromate algae	*? Gandinella or ? Aulotortus friedli,* aulotortus spp., nodosariids, *Agathammina austroalpina, "Sigmoilina" schaeferae* [Late Carnian to Norian-Rhaetian?]	Reddish limestone clasts or pebbles (types 2 and 3) Locality 5	Shoal—Sand bar
Oolitic-coated grains packstone-grainstone (MF 15)	Kumagawa (r) and Itsuki areas (r)	*Major*: ooids and coated grains *Subordinate*: algal fragments, aggregate grains, intraclasts, peloids, grapestones, fragments of crinoids and echinoids, brachiopod shells, few benthic foraminifers and some indeterminable sparite-filled bioclasts	*? Gandinella or ? Aulotortus friedli,*and aulotortids [Upper Triassic]	Grey to light grey limestone breccia or limestone pebbles (types 2 and 3) Localities 5, 11 and 17	Shoal—Sand bar
Radiolarian mudstone-wackestone (MF 16)	Kumagawa (c) and Itsuki areas (c)	*Major*: radiolarians *Subordinate*: thin-shelled bivalves, calcareous nannoplankton and rare crinoid fragments	Late Carnian to Early Norian radiolarians, Nishizono (1996)	Massive grey to light grey bedded limestone intercalated between bedded chert Localities 3, 6, 16, and 19	Basin
Thin-shelled bivalve wackestone-packstone (MF 17)	Kumagawa (c) and Itsuki areas (r)	*Major*: thin-shelled bivalves *Subordinate*: radiolarians, calcareous nannoplankton, and rare intraclasts	Triassic bivalves: *Halobia* and *Danonella* Late Carnian to Early Norian radiolarians, Nishizono (1996)	Massive grey to light grey bedded limestone intercalated between bedded chert Localities 3, 6, 16, and 19	Basin

a abundant, *c* common, *r* rare

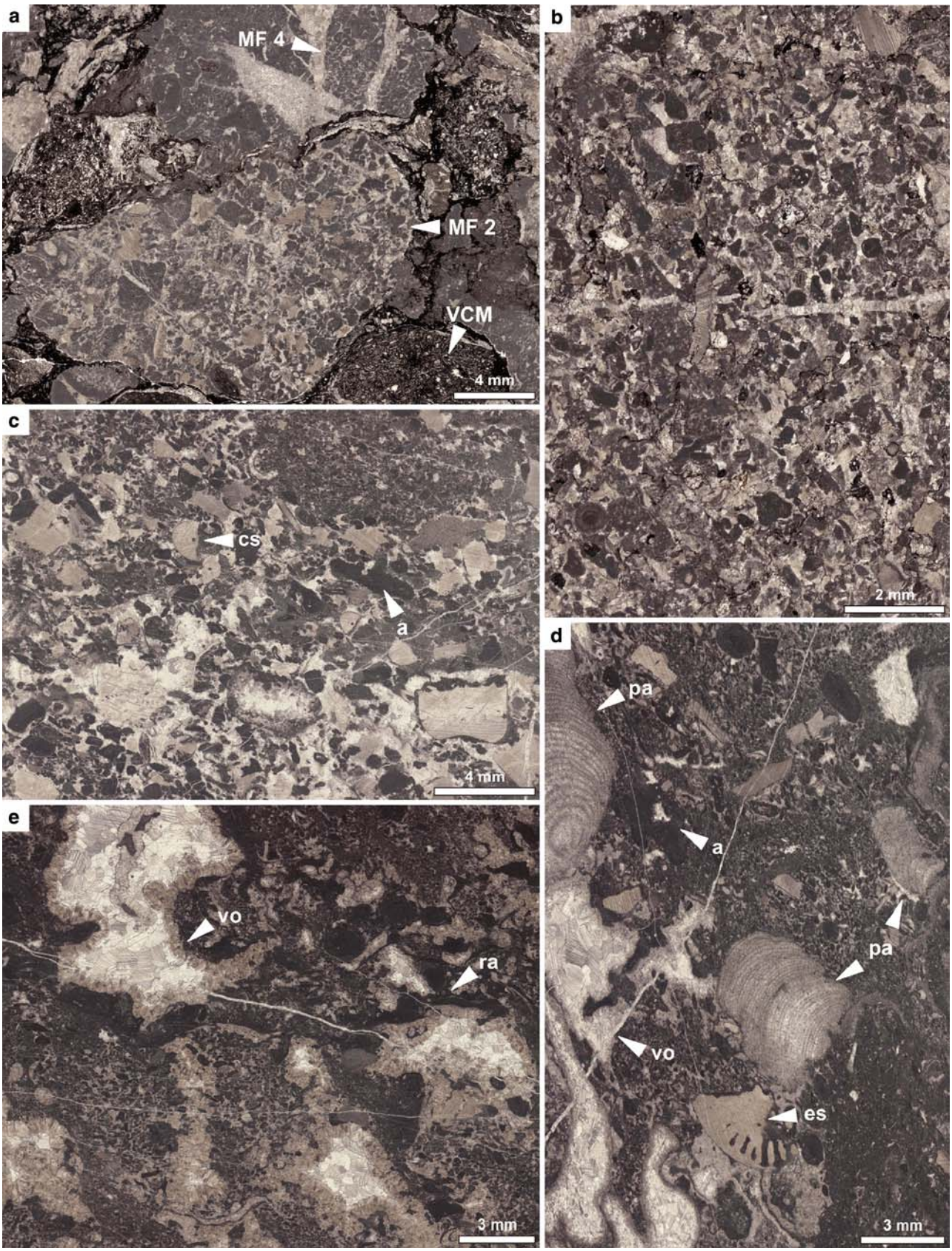
a
MF 4
MF 2
VCM
4 mm
b
2 mm
c
cs
a
4 mm
d
pa
a
pa
vo
es
3 mm
e
vo
ra
3 mm

◀ **Fig. 6** Microscopic views of MF 1 to MF 3. **a** MF 1 (slope), limestone microbreccia with a polymictic clast association of shallow-water limestones, including MF 2 and MF 4, supported by a heavily stylolitized volcaniclastic matrix VCM (JC-Pi 4). **b** MF 1 (slope), fine microbreccia including clasts of 2 mm to small grains (e.g., fragments of echinoderms) of less 1 mm in size ("calciturbidite"), supported by a fine volcaniclastic matrix (JC-DFO 7). **c** MF 2 (fore-reef to slope), crinoidal-algal packstone-grainstone with abundant crinoid stems (*cs*) and fragments of algae (*a*) (JC 91). **d** MF 3 (reef), reef facies including here *Parachaetetes* sp. (*pa*), fragments of algae (*a*), echinoid spine (*es*) and large voids filled by a drusy calcite cement (*vo*). Components are supported by peloidal-bioclastic packstone-grainstone (JC 83). **e** MF 3 (reef), reef facies characterized here by red algae (*ra*) and numerous interstitial voids (*vo*) filled by a drusy calcite cement. All are supported by a peloidal-bioclastic packstone-grainstone (JC 81)

upon the crusts and sparry mosaic cement fills the residual voids. Most of the interstitial cavities in this boundstone are filled either by peloidal-bioclastic wackestone-grainstone or by fibrous isopachous cements.

A detailed description of the reefal facies was given by Onoue and Stanley (2008), who recognized seven microfacies types in the reef locality of Kamase corresponding to the locality 14 in the present paper.

MF 4: Peloidal-aggregate-bioclastic packstone-grainstone (Figs. 7e, 11h, i)

Grey to light grey limestone breccia or limestone pebbles (types 2 and 3). Peloids, aggregate grains, algal debris and coated grains are the main components. Peloids and algal remains (20 to maximum 40%) are subangular to well rounded, poorly sorted, and randomly oriented. Aggregate grains are composed of peloids, algal debris, and some echinoderm fragments. They are 0.5–3 mm in size and represent 10–20% of the rock volume. Subordinate components include porostromate oncoids, tubular algae, bivalve shells, gastropods, echinoids spines, crinoid debris, rare ooids, sponges, corals, and benthic foraminifers including duostominids, aulotortids, and rare *Glomospira* sp., *Glomospirella* sp., "*Textularia*" sp., *Gsolbergella spiroloculiformis*, *Ophthalmidium* sp., *Endotriada* sp. and *Endoteba* sp.. Some extraclasts of biopelmicrite similar in texture of MF 8 to MF 13 can be observed. The matrix is coarse sparry calcite, rarely micritic. The cement is drusy calcite; sometimes thin isopachous fibrous cement can be observed around particles. Most of the skeletal grains, especially echinoderm fragments, show a thin to large micritic rim.

MF 5 Calcimicrobial grainstone (Figs. 7d, 11f, g)

Grey to light grey limestone breccia or limestone pebbles (types 2 and 3). This grainstone is mainly composed of large green algae or cyanobacteria fragments including the porostromate *Garwoodia* and the tubular *Cayeuxia*. Green algae debris is well to moderately sorted, randomly oriented and represents 30–50% of the rock volume. Calcimicrobes are 0.5–1 cm in size. Generally, they form millimeter- to centimeter-sized bushy masses, radial fans, or tangled masses, commonly composed of small tubes or irregularly shaped bodies. The classification of calcimicrobes is based on growth forms and filament patterns. The genus *Cayeuxia* is characterized by branching clusters of tubes, in comparison to the genus *Garwoodia*, which is generally composed of coarse, thin-walled, radiating clusters of tubes. Subordinate components include peloids, algal fragments, aggregate grains, echinoderm fragments, and rare benthic foraminifers, especially duostominids. Aggregate grains are essentially composed of green algae debris and peloids. Drusy sparite cement is abundant, along with large isopachous fibrous cement around components.

MF 6: Mudstone

Light to dark grey massive limestone blocks or limestone breccia (types 1 and 2). This facies corresponds to very fine grained homogeneous micrite lacking coarse bioclasts. Subordinate components include ostracods, peloids, and rare small skeletal grains. This micrite to biomicrite is intensively fractured, and fractures are filled by drusy calcite cement. Stylolites form irregular anastomosing sets. Grains of micrite are generally blocky, ranging in size from 3 to 10 μm.

MF 7: Endotebid mudstone (Figs. 8b, 11k, q)

Thin-bedded dark limestones. Mudstone essentially composed of a rich association of the agglutinated benthic foraminifers *Endoteba* ex. gr. *controversa* and *Endotriada thyrrenica*. Associate components, less than 10% in rock volume, are benthic foraminifers such as small aulotortids (*Aulotortus tenuis*), *Ammodiscus* sp., *Triadodiscus eomesozoicus*, *Ophthalmidium* sp., *Paraophthalmidium* sp., *Duostomina* sp., "*Textularia*" sp., *Agathammina austroalpina*, *Gsolbergella spiroloculiformis*, and nodosariids (*Fondicularia woodwardi*). Small gastropods, ostracods, thin bivalve shells and uncommon echinoderm fragments are subordinated. The matrix is a dark micrite mingled with black pyrite. Abundant framboidal pyrite, incorporated in the micritic matrix, is observable by SEM. Some pyritic solution seams are also visible in thin-sections. Foraminifer chambers are filled by fine-grained equigranular calcite cement, but most foraminifers have been partially replaced by pyrite. In the locality 17, MF 7 commonly occurs at the base of megalodont floatstone (MF 8).

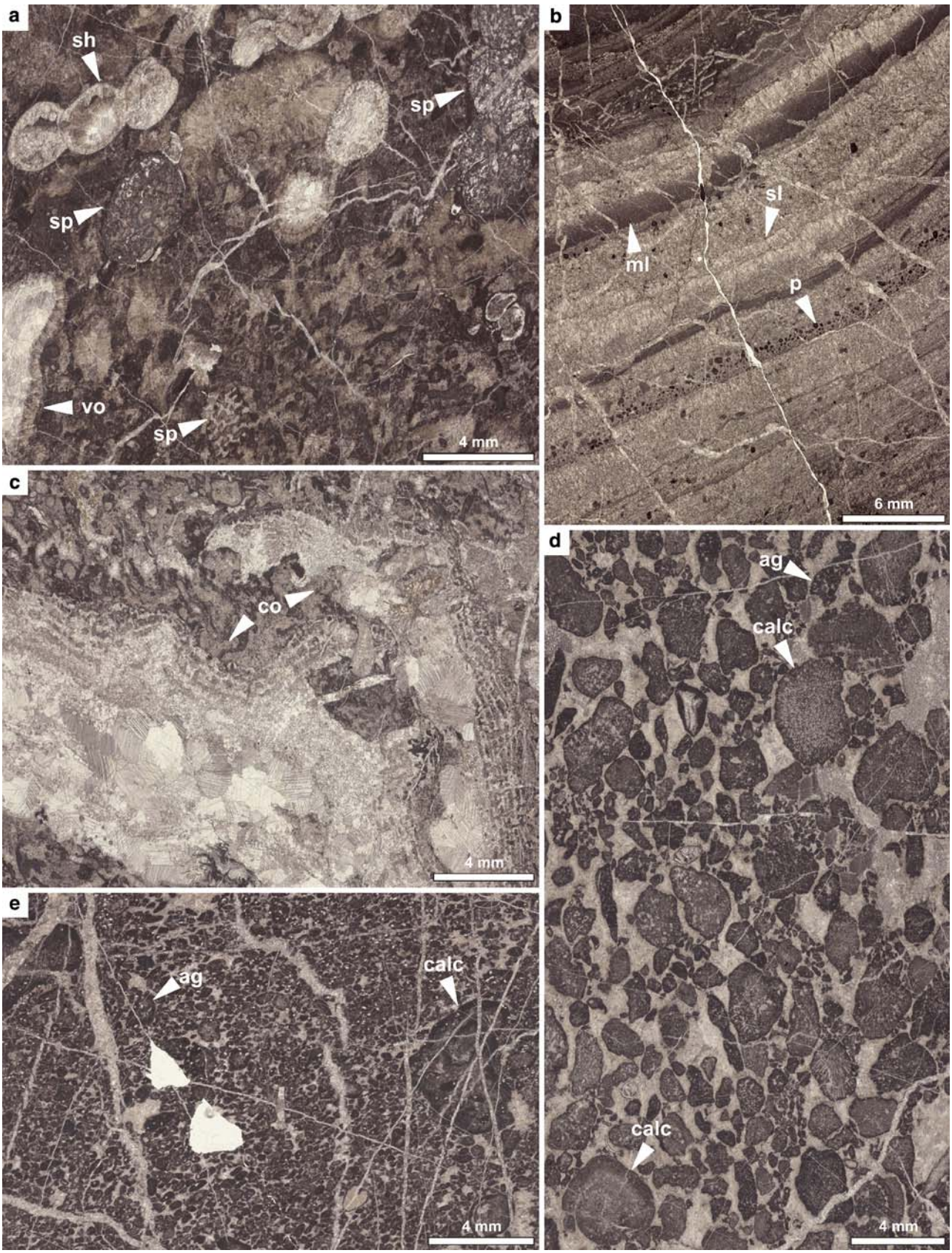
a
sh
sp
sp
vo
sp
4 mm
b
sl
ml
p
6 mm
c
co
4 mm
d
ag
calc
calc
4 mm
e
ag
calc
4 mm

◀ **Fig. 7** Microscopic views of MF 3 to MF 5. **a** MF 3 (reef), reef facies characterized here by spongiomorphids (*sp*), sphinctozoan sponges (*sh*) and voids filled by drusy calcite cement (*vo*). Interstices between components are filled with peloidal-bioclastic packstone-grainstone (JC 88). **b** MF 3 (reef), reef facies characterized here by a stromatolitic microbial bindstone. Microbial lamination is composed of an alternation of micritic (*ml*) and coarse-sparry calcite laminae (*sl*). Micritic and sparitic laminae contain a small amount of peloids (*p*) (JC 32). **c** MF 3 (reef), reef facies composed here of coral section (*co*) with internal tabular structures. Spaces between corals are filled by peloidal-bioclastic packstone-grainstone (JC 84). **d** MF 5 (back-reef to lagoon), calcimicrobial grainstone mainly composed of calcimicrobes (*calc*) including *Garwoodia* and *Cayeuxia* genera, and aggregate grains (*ag*). The rest consist of peloids and fragments of algae, cemented by coarse sparry calcite with isopachous fibrous calcite cement around components (JC-DFO 9A3a). **e** MF 4 (back-reef to lagoon), fine-grained peloidal-aggregate-bioclastic packstone-grainstone largely composed of sorted peloids together with sporadic, coarser aggregate grains (*ag*), coated grains, and calcimicrobe oncoids (*calc*), all cemented by microsparite (JC-DFO 9C)

MF 8: Megalodont floatstone (Figs. 8a, c, 11s)

Grey to dark grey massive limestone blocks (type 1). MF 8 corresponds to floatstone with large megalodont shells locally in life position. The equal-sized bivalves may become several tens of centimeters in size, as is typical for megalodonts of Norian-Rhaetian age, such as *Triadomegalodon* sp. and *Dicerocardium kuwagataforme* (Tamura 1983). Megalodont shells in the outcrop can reach 30–40% of the rock volume. Subordinate components are debris of bivalves, gastropods, benthic foraminifers aulotortids and nodosariids, echinoids, crinoids, ostracods, peloids, microcoprolites, and indeterminable sparite-filled bioclasts. Burrows are common in this facies. The matrix supporting the different skeletal grains is micritic.

MF 9: Echinoderm-bioclastic wackestone-packstone (Figs. 8d, 11r)

Dark grey to grey massive limestone blocks or limestone breccia (types 1 and 2). Wackestone-packstone mostly composed of echinoid spines and crinoid debris. Echinoderm fragments range in size from 0.5 to 1 cm and represent 10–20% of the rock volume. Subordinate components include skeletal coarse-grains, mainly gastropods, aulotortid foraminifers, fragments of large megalodont shells, holothurian sclerites, sponge spicules, rare ostracods and unidentified sparite-filled bioclasts. The matrix is homogenous micrite.

MF 10: Aulotortid packstone (Figs. 8e, 11t-y)

Grey to dark grey massive limestone blocks or limestone breccia (types 1 and 2). This packstone is mainly composed of aulotortid foraminifers including *Aulotortus* ex. gr. *sinuosus*, *A. communis*, *A. tenuis*, and *Auloconus permodiscoides* together with elongate nodosariids (*Frondicularia woodwardi*) and *Agathammina austroalpina*. The content of aulotortids is between 10 and 20%, rarely 50%. Most of the aragonite tests of aulotortids are replaced or filled by sparry calcite, hiding the identification of the internal structures. However, a poorly preserved specimen of ?*Triasina hantkeni*, marker of Late Norian (Sevatian) to Rhaetian, has been identified. The presence of *Triasina hantkeni* along the Kumagawa River has been confirmed in samples of F. Kobayashi (pers. comm. 2008). Subordinate components are bivalve shell fragments (essentially megalodonts), gastropods, ostracods, echinoid and crinoid fragments, serpulids, benthic foraminifers other than aulotortids, especially duostominids, rare peloids and unidentified sparite-filled bioclasts. The matrix is micritic with microcrystalline mosaic calcite often recrystallized to form patches larger than 20 μm. The fracturation is commonly high in this facies.

MF 11: Coprolite-bioclastic wackestone-packstone (Fig. 9a)

Dark grey massive limestone blocks to limestone breccia (types 1 and 2). Wackestone-packstone is mainly characterized by the abundance of crustacean microcoprolites, burrows, and debris of bivalve shells (megalodonts). Well-preserved microcoprolites, produced by crustacean Decapoda were recently identified (Senowbari-Daryan et al. 2009) including two new species, *Payandea japanica* and *Favreina tosaensis*, and one uncertain species *Parafavreina*? sp. Contents of microcoprolites reach 10 to a maximum of 20% in thin-sections. Subordinate components include benthic foraminifer aulotortids and nodosariids, peloids, gastropods, ostracods, echinoderm fragments, and unidentified sparite-filled bioclasts. The matrix is micrite with important fracturation.

MF 12: Molluscan-burrowed wackestone (Figs. 9b-c, 11z)

Dark to grey massive limestone blocks or limestone breccia (types 1 and 2). Wackestone mainly composed of bivalves and their tiny fragments, common burrows and large peloids. The largest bivalve shells are 0.5–5 mm thick and between 1 and 10 cm long. Burrows are commonly associated and filled with large rounded or stretched dark clasts of maximum 1 mm in diameter (e.g., fecal pellets). Voids in burrows are filled by a drusy sparite, which supports peloids. In comparison with MF 11, no microcoprolites with internal structures were observed. Associate components are gastropods, ostracods, smaller benthic foraminifers including *Endotriada* sp., *Endoteba* sp., *Agathammina austroalpina*, few aulotortids and nodosariids, together

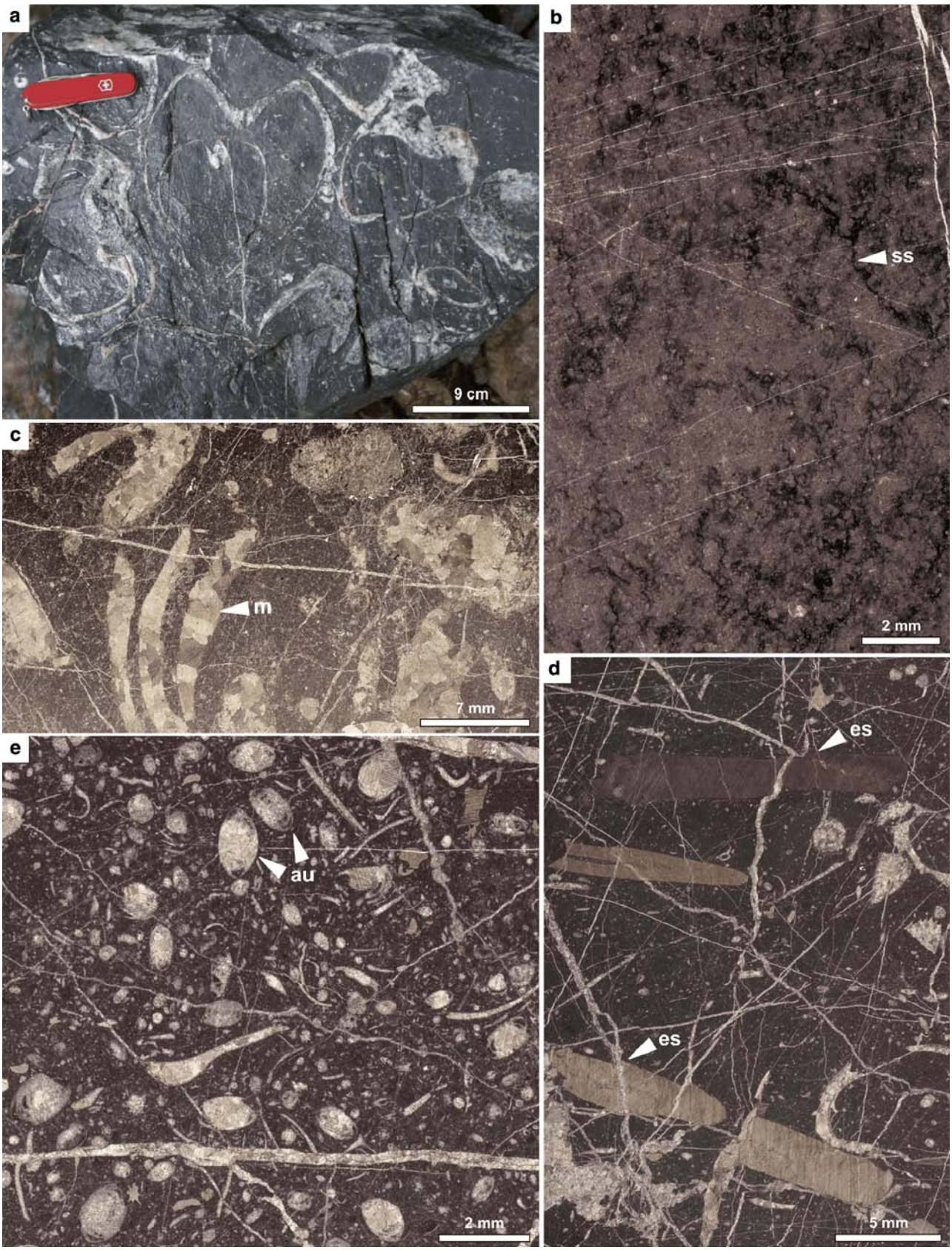
a
9 cm
b
ss
2 mm
c
m
7 mm
d
es
es
5 mm
e
au
2 mm

◀ **Fig. 8** Macro- and microscopic views of MF 7 to MF 10. **a** MF 8 (lagoon), megalodont floatstone with centimetric megalodont shells. Outcrop picture from locality 17, Motoidani Gully. **b** MF 7 (lagoon), Endotebid mudstone consisting of micritic matrix with the benthic foraminifers *Endoteba* ex. gr. *controversa* and *Endotriada thyrrenica*. *Black color* is from pyrite, replacing organic matter. Matrix contains many disintegrated framboidal pyrite and some pyritic solution seams are visible (*ss*) (JC 123). **c** MF 8 (lagoon), megalodont floatstone rich in recrystallized megalodont shells (*m*). Other components are recrystallized bioclasts and peloids supported by micritic matrix (JC 129b). **d** MF 9 (lagoon), echinoid-bioclastic wackestone-packstone composed of large echinoid spines (*es*), with subordinate gastropods and finer skeletal debris, all set in a micritic matrix. This facies commonly occurs associated with MF 8 (JC 40). **e** MF 10 (lagoon), aulotortid packstone mostly composed of aulotortid foraminifers (here, *Aulotortus* ex. gr. *sinuosus*) within a micritic matrix. This facies, associated with MF 8, characterizes the lagoonal setting (JC 26)

with indeterminable sparite-filled bioclasts. The matrix is micrite with grains ranging in size from 3 to 10 μm.

MF 13: Peloidal-bioclastic packstone-grainstone (Fig. 9d)

Dark grey to grey massive limestone blocks or limestone breccia (types 1 and 2). Packstone-grainstone mostly composed of peloids and skeletal debris. Peloids are small in size, rarely exceeding 200 μm. They are partly subangular and contribute to 20–40% of the rock volume. Skeletal grains are poorly sorted, randomly oriented, and generally well rounded. Subordinate components are algal fragments, bivalves, gastropods, crinoids and echinoids, ostracods, few ooids, rare benthic foraminifers including nodosariids, aulotortids and duostominids, as well as unidentified sparite-filled bioclasts. Ooids are generally ellipsoidal with peloids acting as nuclei. The matrix is predominantly micritic, rarely sparitic. Isopachous fibrous cement occurs and the remaining voids are filled by drusy sparite. The main difference between MF 13 and MF 4 is basically the composition. MF 13 does not show aggregate grains and calcimicrobes.

MF 14: Foraminiferal grainstone (Fig. 9se, 11aa-dd)

Reddish limestone clasts or pebbles (types 2 and 3). Grainstone mostly composed of benthic foraminifers including abundant uncertain specimens which could belong to the genus *Gandinella*, as well as to the species *Aulotortus friedli*. A precise systematic description is needed here to assume the belonging of these specimens (work in progress). Associate foraminifers are *Aulotortus* spp., *Agathammina austroalpina*, "*Sigmoilina*" *schaeferae*, and a few nodosariids. Content of foraminifers varies between 30 and 50%. A large amount of these foraminifers show truncated test with a pressure solution contact. Subordinate components include coated grains, ooids, peloids, bivalve shells fragments, gastropods, algal debris, crinoids, echinoids, and rare debris of calcimicrobes. The ooids are generally micritic and most of skeletal grains, specifically peloids, algal remains and some foraminifers, are coated. The matrix is a sparry calcite. Cement around grains and foraminifers is primary isopachous fibrous and become drusy sparite in wider spaces.

MF 15: Oolitic-coated grains packstone-grainstone (Fig. 10a-b)

Grey to light grey limestone breccia or limestone pebbles (types 2 and 3). This facies corresponds to packstone-grainstone characterized by abundant ooids and coated grains. Ooids (20–40%) show concentric layering and some features, possibly relicts of radial structures. They are predominantly round shaped and their size ranges from 0.2 to 1 mm. Peloids, algal fragments, echinoderm debris, intraclasts, aggregates or grapestones are the main nuclei of ooids and components of coated grains. Associate components are algal fragments, aggregate grains, grapestones, fragments of crinoids and echinoids, brachiopod shells, benthic foraminifers (same specimens of MF 14), and some unidentified sparite-filled bioclasts. Aggregate grains are composed of algal debris and peloids. Grapestones correspond to an amalgamation of concentric ooids. Echinoderm fragments show a thin micritic rim. The matrix is generally sparite including some relics of micrite. Drusy sparite cement occurs, as well as fibrous cement observable around ooids and grains. In some cases, residual mud is incorporated within the sparry calcite cement.

MF 16: Radiolarian mudstone-wackestone (Fig. 10d)

Massive grey to light grey bedded limestone intercalated between bedded cherts. Abundant radiolarians, more than 50%, and few thin-shelled bivalves are the biogenic components. Some crinoid fragments can be present. Matrix is homogenous micrite. The radiolarian tests are commonly dissolved and filled by sparite. Details on taxonomy of these Late Carnian to Early Norian radiolarians are given in Nishizono (1996). Calcareous nannoplankton was reported by Onoue and Sano (2007) in the micritic matrix.

MF 17: Thin-shelled bivalve wackestone-packstone (Fig. 10c)

Massive grey to light grey bedded limestone intercalated between bedded cherts. It corresponds to wackestone-packstone with abundant thin-shelled bivalves (filaments), radiolarians, and rare intraclasts. Thin-shells range in size from 10 to 100 μm thick and 0.5–5 mm length. They

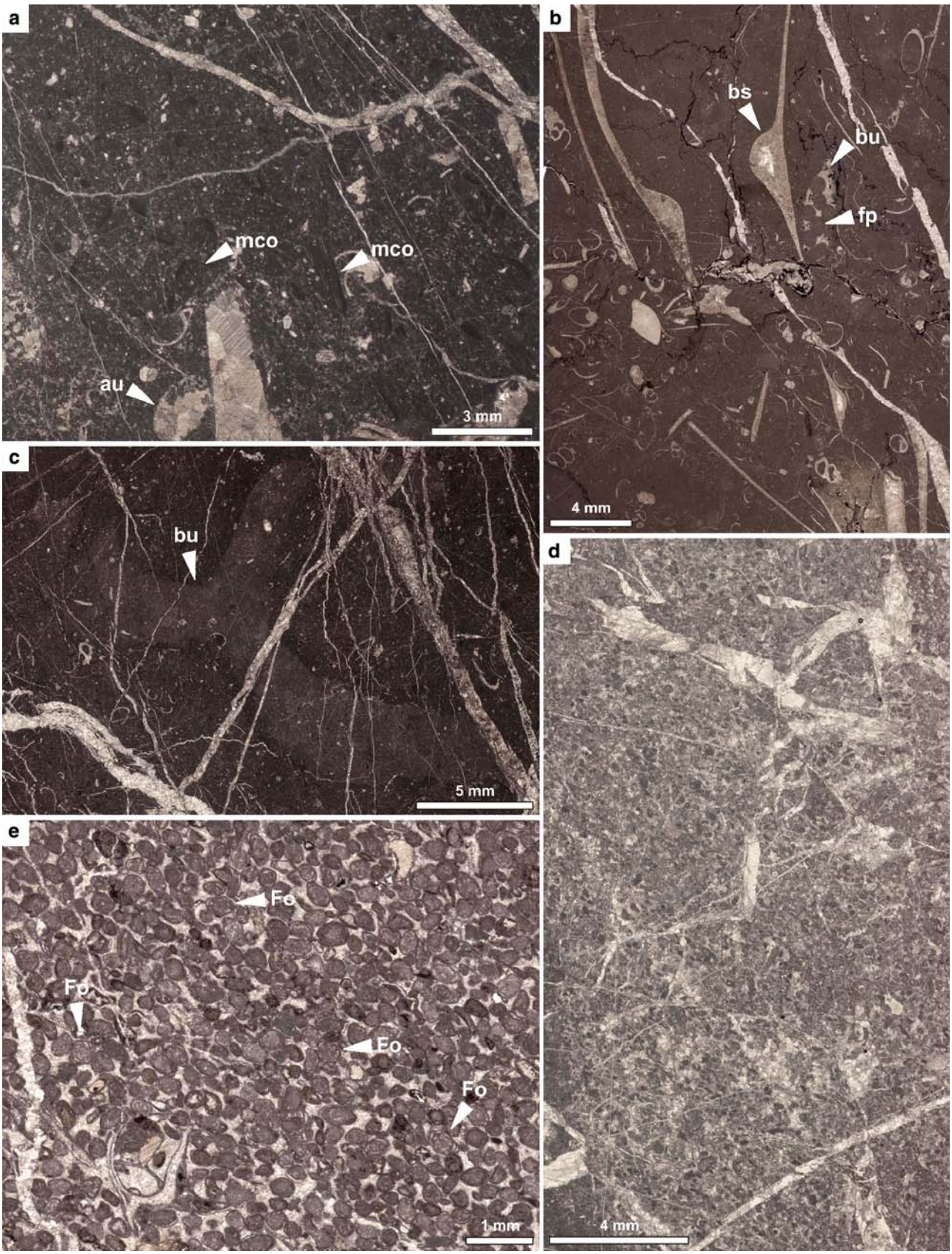
a
mco
mco
au
3 mm
b
bs
bu
fp
4 mm
c
bu
5 mm
d
4 mm
e
Fo
Fp
Eo
Fo
1 mm

◀ **Fig. 9** Microscopic views of MF 11 to MF 14. **a** MF 11(lagoon), coprolite-bioclastic wackestone-packstone composed of the micro-coprolite (*mco*) *Payandea japanica* (Senowbari-Daryan et al. 2009). The rest are recrystallized aulotortids (*au*) and bioclasts supported by micritic matrix (JC 129a). **b** MF 12 (lagoon), molluscan-burrowed wackestone composed of numerous bivalve shells (*bs*), here aligned, burrow (*bu*) with micritic fecal pellets inside (*fp*) and recrystallized tiny bioclasts supported by micritic matrix (JC-MO 1). **c** MF 12 (lagoon), burrowed bioclastic wackestone with large burrow (*bu*) and tiny recrystallized skeletal debris supported by micritic matrix (JC 125). **d** MF 13 (lagoon), fine-grained peloidal packstone-grainstone mainly composed of peloidal particles supported by the lime-mud, or filled by microsparite (JC 67). **e** MF 14 (shoal-sand bar), foraminiferal grainstone, exclusively composed of foraminifers (*Fo*) related to the genus *Gandinella* or species *Aulotortus friedli* and few aulotortids, all cemented by sparry calcite (JC-Pi 1b)

represent 20–40% on average, and exceptionally 60%. They are generally well sorted and disposed parallel to each other. Thin-shelled bivalves belong to the genera *Halobia* and *Danonella* (Kanmera 1969). Calcareous nannoplankton from the micritic matrix was reported by Onoue and Sano (2007).

Facies interpretation

In the present chapter, all the microfacies are interpreted separately according to their depositional environment. As the samples were taken in dismantle limestones, including blocks, breccias, and pebbles within a volcaniclastic or mudstone matrix; the facies succession, both laterally and vertically, remains largely uncertain. Furthermore, our Upper Triassic foraminiferal control is not precise enough to obtain a fine biostratigraphic timing of the facies succession, in order to drawn a columnar section illustrating the mutual stratigraphic relation of facies types recognized.

Slope

MF 1 corresponds to a limestone microbreccia facies, which mostly consists of clasts originating from shallow-water settings, and contains subsequently different microfacies types (e.g., lagoon, shoal, back-reef, and reef). These lithified clasts show locally a grading in grain size, suggesting that MF 1 is probably a gravitational deposit, originating from shallow-water sediments from the flanks of the atoll-type to deeper settings of the slope. According to the grain size, we distinguish different levels of breccia, from the coarse debris flow (centimetric clasts) to possible calciturbiditic deposits (millimetric grains), characterized by small laminations on the outcrop and by a granoclassement (locality 5, Ose, Fig 4). This slope environment, characterized by such debris flow or eventually turbidites, corresponds to the transition from the shallow-water platform margin to the toe of seamount. Supposedly, such deposits could form during the sedimentation of atoll-type carbonates (Mullins and Cook 1986), and not only after the major tectonic dismantling of the seamount.

Fore-reef

MF 2 is a coarse-grained facies containing components (crinoids, echinoids, and algal fragments) characteristic of a fore-reef environment adjacent to a sponge-coral-algal reef (Becker and Dodd 1994). The fore-reef facies observed here generally present a mass accumulation of crinoids, which commonly occurs in the reef flank beds due to transport and deposition of autochthonous as well as parautochthonous remnants (Michalik et al. 1993; Flügel 2004). The foraminiferal assemblage of *Duostomina* sp. and *Variostoma* sp. indicates open-marine conditions in agreement with a fore-reef setting.

Reef

MF 3 is sponge-coral-algal boundstone, including also some laminated stromatolites or spongiomorpha. According to components and field observations (locality 14 in Fig. 4), MF 3 is interpreted as reef deposits. This reef could be either a patch-reef (Onoue and Stanley 2008) in a lagoonal setting or occurring on a bank margin around seamount, on a windward edge. The presence of microbial laminations involves generally low-energy conditions in comparison to the high energy typical in a reef front or reef rim where corals, sponges, and algal frame-builders principally grow. In our samples, the presence of scleractinian corals and calcareous sponges preserved in situ (Kanmera 1969; Onoue and Stanley 2008) suggests that they formed an organic framework in a shallow subtidal setting. The grain-supported fabric and the well-sorted nature of skeletal components in the peloidal-bioclastic wackestone-grainstone facies indicate high-energy conditions in this shallow subtidal environment, as typical for framework reef elsewhere (Onoue and Stanley 2008). Most of the bioclastic fragments are well rounded, indicating redeposition.

The interstitial cavities of the corals, sponges, and microbial encrusters are locally cemented by isopachous fibrous to drusy calcite cements, suggesting active water circulation and submarine cementation. Cavities can also be filled by peloidal-bioclastic wackestone-grainstone. The extensive water circulation around the sponge-coral-algal reef enhanced submarine syndepositional growth of radiaxial-fibrous calcite that contributed to an early lithification of the sediment (Onoue and Stanley 2008). Furthermore, water circulation across a reef margin in the context of an atoll can be enhanced by cross-reef currents and tidal exchange (Atkinson et al. 1981).

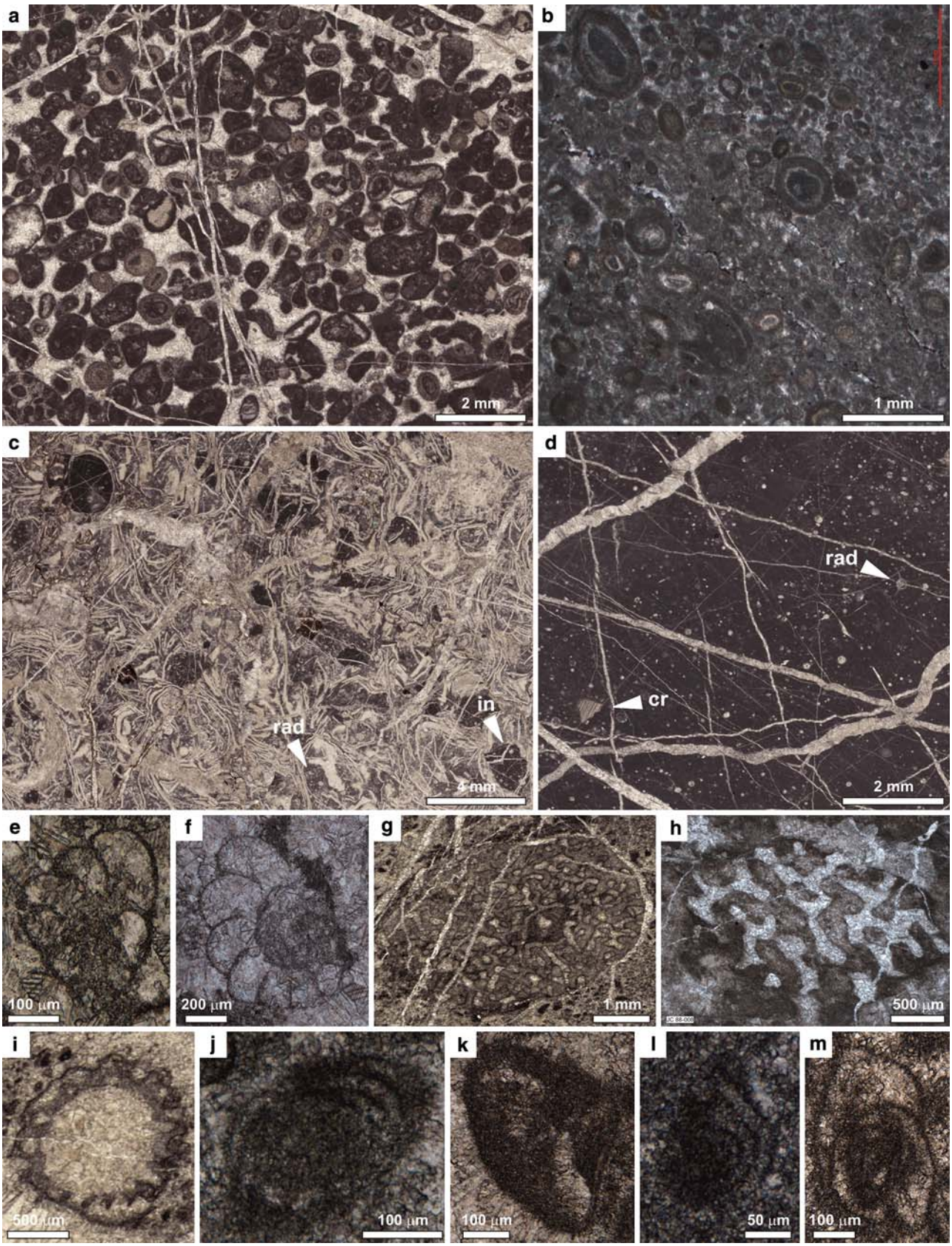
a
2 mm
b
1 mm
c
rad
in
4 mm
d
rad
cr
2 mm
e
100 μm
f
200 μm
g
1 mm
h
500 μm
i
500 μm
j
100 μm
k
100 μm
l
50 μm
m
100 μm

◀ **Fig. 10** Microscopic views of MF 15 to MF 17 and biotic components of fore-reef to reef facies, including benthic foraminifers. **a** MF 15 (shoal), oolitic-coated grains grainstone chiefly composed of concentric ooids with radial structures in place, and coated grains (peloids, intraclasts, echinoderms). Subordinate are fragments of algae and calcimicrobes supported by coarse sparry calcite (JC 64b). **b** MF 15 (shoal), oolitic-coated grains packstone-grainstone with concentric ooids, coated grains and peloids supported by micritic matrix (JC-DFO 2). **c** MF 17 (basin), thin-shelled bivalve packstone essentially composed of filaments supported by the micritic matrix rich in radiolarians (*rad*). Some intraclasts are present (*in*) (JC 44). **d** MF 16 (basin), radiolarian mudstone principally contains radiolarians (*rad*), often associated with thin-shelled bivalves (not present here). Radiolarians and other bioclasts like crinoids (*cr*) are supported by the micritic matrix (JC 46). **e** MF 1 (fore-reef), *Variostoma* sp. (JC 80). **f** MF 1 (fore-reef), *Diplotremina* sp. (JC 16). **g** MF 3 (reef), spongiomorphid (JC 83). **h** MF 3 (reef), spongiomorphid (JC 88). **i** MF 3 (reef), dasycladacean alga (JC 87). **j** MF 3 (reef), *Glomospira* sp. (JC 81). **k** MF 3 (reef), *Hirsutospirella* cf. *pilosa* (JC 61). **l** MF 3 (reef), *Ophthalmidium* cf. *exiguum*. (JC 83). **m** MF 3 (reef), *Galeanella panticae* (JC 62)

The biostratigraphic range of MF 3 is Late Carnian to Rhaetian with different stages in the reef growth evolution, according to the biotic association of corals and/or sponges. The reefal shallow-water carbonate sedimentation was initiated in Late Carnian time with typical Carnian-age corals such as *Craspedophyllia ramosa*, *Craspedophyllia gracilis*, and *Volzeia badiotica* (Kanmera 1964; Onoue and Stanley 2008). Furthermore, the sponge community represents a mixed Late Carnian-Norian fauna (Senowbari-Daryan, pers. comm. 2008), suggesting that the main reef building took place during the Late Carnian to Norian. For this reason, we postulate that *Retiophyllia* frame-built reefs, always associated with sponge bafflestone, developed during the Late Norian to Rhaetian according to the overall composition and evolution of reefs in the western Tethys (Flügel 2002). A new discovery of a large reefal succession with a patch of *Retiophyllia* sp. at the Inaba cave (Shikoku Island) confirms this assumption (Onoue et al. 2009). Most of the coral species described by Kanmera (1964) and Onoue and Stanley (2008) show a close affinity to these of the Norian and Rhaetian Zlambach beds of Austria and the Upper Triassic of Timor.

The foraminiferal assemblage of MF 3, including *Agathammina austroalpina*, *Glomospira* sp., *Hoyenella inconstans*, *Endotriada thyrrenica*, and *Galeanella panticae*, confirms the Late Carnian–Rhaetian biostratigraphic range of the reef growth. The reefal foraminiferal assemblage of the Sambosan AC is similar to that reported from the Tethys realm and confirms a tropical to subtropical condition during the deposition of these limestones.

Back-reef: lagoon

MF 4 and MF 5 are characterized by aggregates grainstone corresponding to different particles that have been agglutinated to form compound grains. It involves microbial binding and is precisely associated with calcimicrobes (MF 5). These films or mats are generally found in lower-energy, shallow-water settings, such as lagoons. In our samples, the calcimicrobes (*Cayeuxia* and *Garwoodia*) occur as fragments reworked from lower-energy lagoonal areas to higher-energy zones such as back-reef.

Porostromate algae and cyanobacteria are common constituents of open and restricted lagoonal environments (Kiessling and Flügel 2000).

The subordinate aggregate grains range from lump to mature lump stage (Flügel 2004). Well known in the Late Triassic deposits, they are common in attached or isolated carbonate platforms. In the present case, the peloidal, grapestones, and cyanobacteria are well sorted and sometimes coated, indicating moderate to high water energy, tropical and subtropical warm-water conditions, low-nutrient environment, and low sedimentation rates. The association of the Porostromata with grapestones characterizes an open-marine lagoon.

Most of the peloids are remains of algae. In MF 4 and MF 5, skeletal grains, especially echinoderm fragments, show a thin to large micritic rim, indicating a back-reef to lagoon environment (Reid 1987). Coral and sponge fragments are rare, whereas microbial components and algal fragments are abundant. The matrix, which mainly corresponds to coarse sparry calcite cement, sometimes with large isopachous fibrous cement, suggests a submarine cementation and an active water circulation.

MF 4 and MF 5 are less well constrained in terms of timing, but the presence of foraminifers including *Duostomina* sp., *Variostoma* sp., *Diplotremina* sp., and rare *Glomospira* sp., *Glomospirella* sp., "*Textularia*" sp., *Gsolbergella spiroloculiformis*, *Ophthalmidium* sp., *Endotriada thyrrenica*, *Endoteba* ex. gr. *controversa* and aulotortids points to a Late Triassic age, with a biostratigraphic range from Late Carnian to Norian. Furthermore, both facies show strong similarities with the Norian-Rhaetian carbonates from the North Palawan also originated on seamounts (see the Oncoid float/grainstone of Kiessling and Flügel 2000: plate 13, Figs. 3, 4).

Lagoon

MF 6 and MF 7 are mud-rich. The important thickness of mud-dominated deposits in the Sambosan AC points to a high subsidence rate of the seamounts or eustatic sea-level changes that, as in modern seamounts lagoon, enable the deposition of a thick sequence. MF 7, which is characterized by dark *Endoteba* and *Endotriada* mudstone, represents the only thin-bedded deposits encountered in the present study. This facies, nearly laminated, occurs at the base of megalodont limestone succession in the locality 17

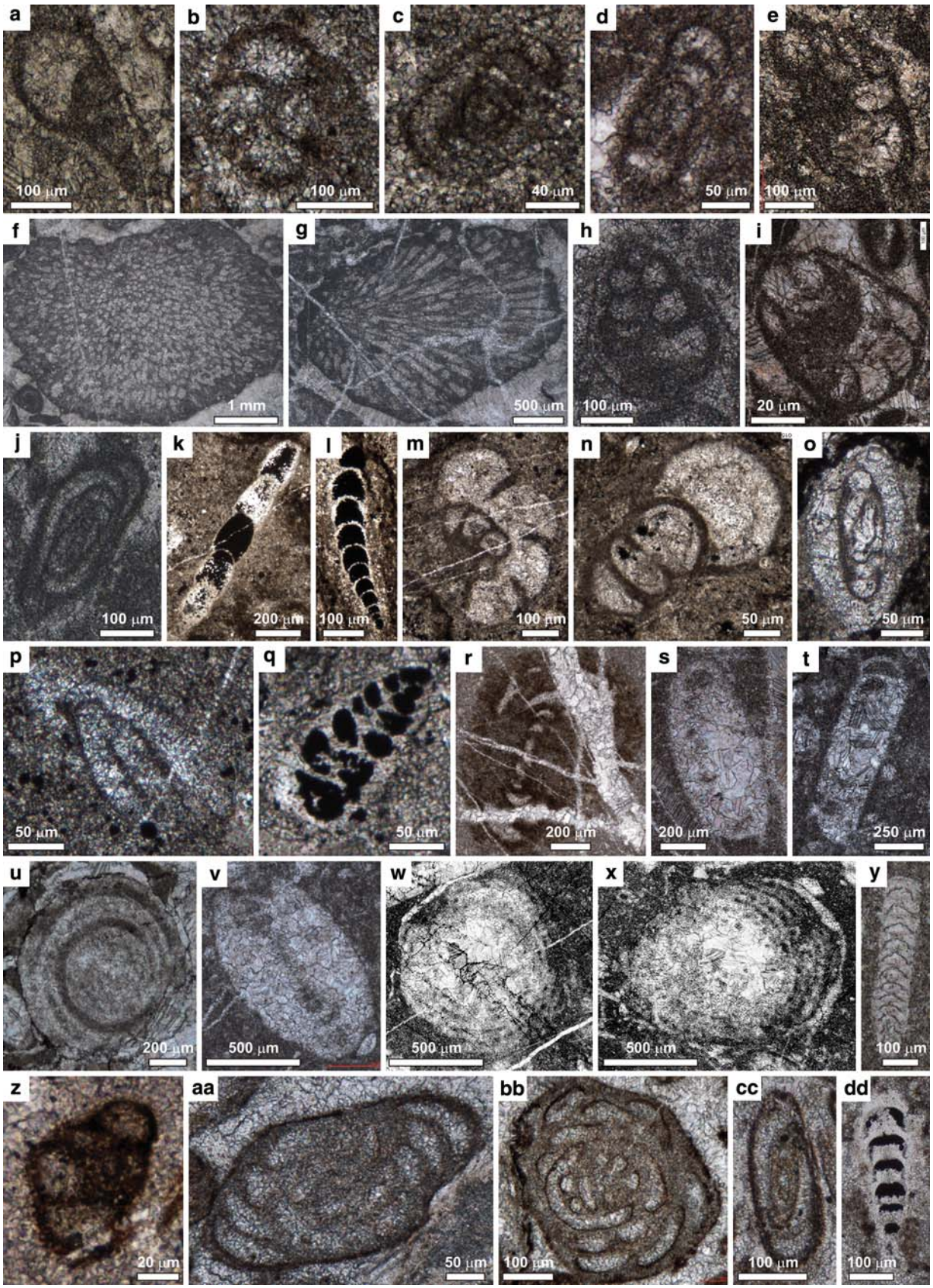
a
100 μm
b
100 μm
c
40 μm
d
50 μm
e
100 μm
f
1 mm
g
500 μm
h
100 μm
i
20 μm
j
100 μm
k
200 μm
l
100 μm
m
100 μm
n
50 μm
o
50 μm
p
50 μm
q
50 μm
r
200 μm
s
200 μm
t
250 μm
u
200 μm
v
500 μm
w
500 μm
x
500 μm
y
100 μm
z
20 μm
aa
50 μm
bb
100 μm
cc
100 μm
dd
100 μm

◀ **Fig. 11** Microscopic views of Upper Triassic benthic foraminifers and calcimicrobes of reef, back-reef, lagoon, and shoal facies. **a** MF 3 (reef), *Planinvoluta* sp. (JC 80). **b** MF 3 (reef), *Endotriada thyrrenica* sp. (JC 88). **c**, **d** MF 3 (reef), *Hoyenella inconstans* (JC 81; JC 77). **e** MF 3 (reef), "*Trochammina*" sp. (JC 87). **f** MF 5 (back-reef to lagoon), calcimicrobe *Garwoodia* sp. (JC_DFO 9A3b). **g** MF 5 (back-reef to lagoon), calcimicrobe *Cayeuxia* sp. (JC-DFO 9A3b). **h** MF 4 (back-reef to lagoon), *Textularia* sp. (JC-DFO 2). **i** MF 4 (back-reef to lagoon), *Variostoma* sp. (JC 58). **j** MF 4 (back-reef to lagoon), *Agathammina austroalpina* sp. (JC_Pi 5a). **k** MF 7 (lagoon), Nodosariidae (JC 123). **l** MF 7 (lagoon), *Frondicularia woodwardi* (JC 123). **m** MF 7 (lagoon), *Endotriada thyrrenica* (JC 123). **n** MF 7 (lagoon), *Endoteba* ex. gr. *controversa* (JC 123) **o** MF 7 (lagoon), *Gsolbergella spiroloculiformis* (JC-MO 9). **p** MF 7 (lagoon), Miliolidae (JC-MO 9). **q** MF 7 (lagoon), "*Textularia*" sp. (JC_MO 9). **r** MF 9 (lagoon), *Aulotortus* ex. gr. *sinuosus* (JC 59). **s** MF 8 (lagoon), *Auloconus permodiscoides* (JC 15). **t** MF 10 (lagoon), *Aulotortus tenuis* (JC 12). **u**, **v** MF 10 (lagoon), *Aulotortus* ex. gr. *sinuosus* (JC 24; JC 15). **w**, **x** MF 10 (lagoon), *Triasina hantkeni* (K-8-6, collected by F. Kobayashi). **y** MF 10 (lagoon), *Frondicularia woodwardi* (JC 19). **z** MF 12 (lagoon), *Agathammina austroalpina* (JC 76). **aa, bb** MF 14 (shoal to lagoon), uncertain foraminifera related to the genus *Gandinella* or species *Aulotortus friedli* (JC 37). **cc** MF 14 (shoal to lagoon), *Agathammina* sp. (JC-DFO 3). **dd** MF 14 (shoal to lagoon), *Austrocolomia* cf. *marshalli* (JC-DFO 10)

(Motoidani Gully), the single one illustrating a stratigraphic succession (Onoue and Tanaka 2005). Some dark solution seams (pyrite) are visible, indicating a late lithification and early compaction of sediments. Furthermore, many framboidal pyrites, incorporated in the micritic matrix, are observable in MF 7 by SEM, suggesting that organic matter originally present in this facies was replaced by pyrite in a reducing environment and, thus, records reducing conditions (Hudson 1982). This type of anoxic environment should be poor in benthos, which is not the case in the present study. A rich assemblage of *Endoteba* spp., *Endotriada* spp., and numerous nodosariids occurs. A recent paper of Beatty et al. (2008) showed oxygenation linked to waves might preclude anoxia in shallow-marine settings. We can easily imagine that this Triassic atoll-type carbonates platform was subject to important wave action or storms.

Biostratigraphically, MF 7 is interpreted to be Late Carnian in age and occurs at the base of the megalodont limestone of Norian to Rhaetian age. It is inferred that this dark mudstone may represent the initial stage of carbonate sedimentation in the Sambosan AC upon the volcanic basement. However, due to the presence of typical Carnian to Norian bivalves (e.g., *Gruenewaldia decussata*, *G. woehrmanni*, and *Paleoneilo elliptica*), and of Middle Norian conodont assemblage (e.g., *Epigondolella multidentata*, *E. medionorica*, *E. spiculata*, and *E. tozeri*) reported by Onoue and Tanaka (2005), the deposition of MF 7 certainly continues until the Norian. The foraminifers association (small aulotortids, *Agathammina austroalpina*, *Gsolbergella spiroloculiformis*, *Frondicularia* sp., and *Ophthalmidium* sp.) is in agreement with this assumption.

MF 8 to MF 12 are characterized by abundant aulotortid foraminifers, gastropods, shell fragments, echinoderm fragments, coprolites, megalodonts, and burrows. These components, specifically megalodonts (Tichy 1975; Tamura 1983), point to a protected lagoonal setting, as observed in many Late Triassic carbonate platforms (Fischer 1964; Martini et al. 1997; Kiessling and Flügel 2000). The occurrence of the foraminifers nodosariids and dusotominids along with aulotortids and megalodonts, indicates connections to the open ocean (Zaninetti 1976). Bioturbation and burrows, common in MF 11 and MF 12, are typical of inner and mid-shelf environments. Burrowed mudstones rich in megalodonts are reported from most contemporaneous carbonate platforms (Fischer 1964; Bernecker 1996; Enos and Samankassou 1998).

The megalodonts floatstone, MF 8, described in the Kumagawa and in the Itsuki areas, indicates a shallow muddy substrate in a low-energy lagoonal environment (Flügel 2004). Most of megalodontid bivalves are Norian in age according to Tamura (1983) and Onoue and Tanaka (2002). The foraminifer assemblage found in MF 8, including numerous aulotortids, *Agathammina austroalpina*, and *Triasina hantkeni*, strengthen the biostratigraphic range of Norian to Rhaetian assumed.

MF 9, rich in echinoid spines, crinoid ossicles, aulotortids, and gastropods, is interpreted as deposited in the lagoon, closely associated or mingled with the megalodonts floatstone. We recently found the same facies associated with large megalodont shells in the Upper Triassic limestones of the Kanto Mountains in Honshu Island, northwest of Tokyo (author's unpublished data).

MF 10 and MF 11, respectively composed of numerous aulotortids and microcoprolites, supports the interpretation as the low-energy lagoonal deposits suggested by MF 6 to MF 9 above. Most of the originally aragonitic foraminifer tests show an early dissolution and a subsequent recrystallization, as reported elsewhere for Aulotortidae (Piller 1978). The recent discovery in MF 11 of the new species microcoprolite *Payandea japanica* from the locality 17 (Senowbari-Daryan et al. 2009) provides new insight into Triassic crustacean microcoprolites paleobiogeography. According to the presence of *Triasina hantkeni* in these facies, a Norian-Rhaetian age is given here.

The molluscan-burrowed wackestone, MF 12, is mainly composed of bivalve shells and burrows. Most of the burrows are filled with large rounded or stretched peloids indicative of fecal pellets. Unfortunately, no internal structures are preserved precluding species determination. A low-energy lagoonal environment is also proposed for this deposit. MF 12 has a Late Carnian to Rhaetian biostratigraphic range. However, it should be noted that this facies was firstly recorded during the Late Carnian to

Norian and secondly through Norian to Rhaetian. Indeed, in locality 17, we recently observed a bioclastic burrowed mudstone level associated with MF 7. Both microfacies, deposited upon volcaniclastic rocks at the base of megalodonts succession, should correspond to the initial stage of carbonate sedimentation. They are composed of bivalve shells and endotebid foraminifers associated with rare Late Carnian corals reworked from the reef, and set generally in volcaniclastic debris. In other localities, MF 12 is composed of shells but associated with aulotortids and megalodont fragments, suggesting in this case a Norian-Rhaetian biostratigraphic range.

MF 13 corresponds to a peloidal-bioclastic packstone-grainstone. Peloids are components that occur in almost all microfacies types. They are not really diagnostic of any particular environment but are the main components of very shallow water subtidal sediments, especially lagoonal sand and muds (Wright and Burchette 1996). Skeletal grains are poorly sorted, randomly oriented, and generally well rounded, indicating transport and redeposition. Isopachous fibrous cement locally occurs, indicating submarine cementation. MF 13 is thought to occur all over the lagoonal unit, but should be more predominant in the outer part of the lagoon commonly associated with a shoal or a back-reef facies. MF 13 has almost the same foraminifer assemblage as MF 4 and MF 5 and points to an Upper Triassic biostratigraphic range.

Shoal: sand bar

MF 14, foraminiferal grainstone, associated with MF 15, oolitic-coated grains packstone-grainstone corresponds to typical coated grains and oolitic facies of shoal-sand bar. These lithofacies are best developed in wave- and tidally influenced areas where water depth is less than 3–5 m. The concentric ooids are indicative of high-energy conditions and normal marine salinity, which is typical of a shoal in shelf-edge or bank margin facies (Blendinger and Blendinger 1989). The isopachous fibrous cement, as well as the gastropod shells, early filled by foraminifera, and the total absence of mud in the foraminiferal grainstone of MF 14 equally indicate a high water-energy environment in assumption with a sand-bar setting. Most of the foraminifers of MF 14 show truncated test with a pressure solution contact, indicating late cementation and early compaction of sediments. The total absence of reefbuilding organisms indicates a far reef position of the depositional environment.

The overall restricted lateral extension of the oolitic and coated grains limestones in Sambosan AC could be explained by a rapid fall in sea level or drowning of the platform that may have stopped the ooid factory (Bosellini et al. 1981). Important storms and debris flows from the shoal to the foot of the seamount might also explain the low occurrence of the coated grains to oolitic facies. The presence of reddish iron impregnated surfaces, especially in MF 14, is interpreted to have formed in a meteoric environment on a shoal, corresponding to the depositional setting. We recently discovered similar ooids bank facies in the islands of Shikoku and Honshu.

The presence of the benthic foraminifers *Aulotortus* spp. associated with *Agathammina austroalpina* in MF 14, confirms a Late Carnian to Norian (-Rhaetian?) biostratigraphic range.

Basin

MF 16 and MF 17, rich in radiolarians and thin-shelled bivalves, are interpreted as pelagic limestone deposited in a basinal environment, where they are intercalated between bedded cherts. Radiolarians and thin-shelled bivalves are common. Neither real vertical change in lithologic features and components nor volcanic sediments were observed, suggesting that these pelagic limestones were deposited in a relatively deep, quiet environment (Kanmera 1969). The presence of calcareous nannoplankton in the micritic matrix of MF 16 and 17, as also observed in the Upper Triassic deeper-water limestone from the Northern Calcareous Alps, India, and northwestern Australia, could explain the origin of the mud (Onoue and Sano 2007; Jafer 1983; Bralower et al. 1991; Rai et al. 2004). Indeed, Onoue and Sano (2007) reported calcareous nannoplanktonic forms in the Sambosan pelagic limestone, suggesting that significant pelagic carbonate accumulation occurred in the Panthalassa as well as in the Tethys Oceans.

Micropaleontologically, the reefal and lagoonal foraminifera assemblage described in MF 2 to MF 15 is important for the biostratigraphy, the paleogeography, and the paleoecology of the Upper Triassic limestones of Japan. All foraminifers revealed by this study show a strong affinity to those of the Tethys realm and confirm the tropical/subtropical conditions during the deposition of the Upper Triassic Sambosan limestones in the Panthalassan Ocean (Chablais et al. 2007, 2008). The presence of typical Triassic, both lagoonal and reefal benthic foraminifers of Tethyan affinity in Japan, indicates that foraminifers might have been widespread all around the world, using numerous possibilities (Alve 1999; Alve and Goldstein 2003; Pawlowski and Holzmann 2008). They seem to be able to colonize different areas if the paleoecologic conditions are met. Biostratigraphically, the foraminifers indicate a Late Carnian to Rhaetian age for the Sambosan limestones, with the main lagoonal carbonate production during the Norian.

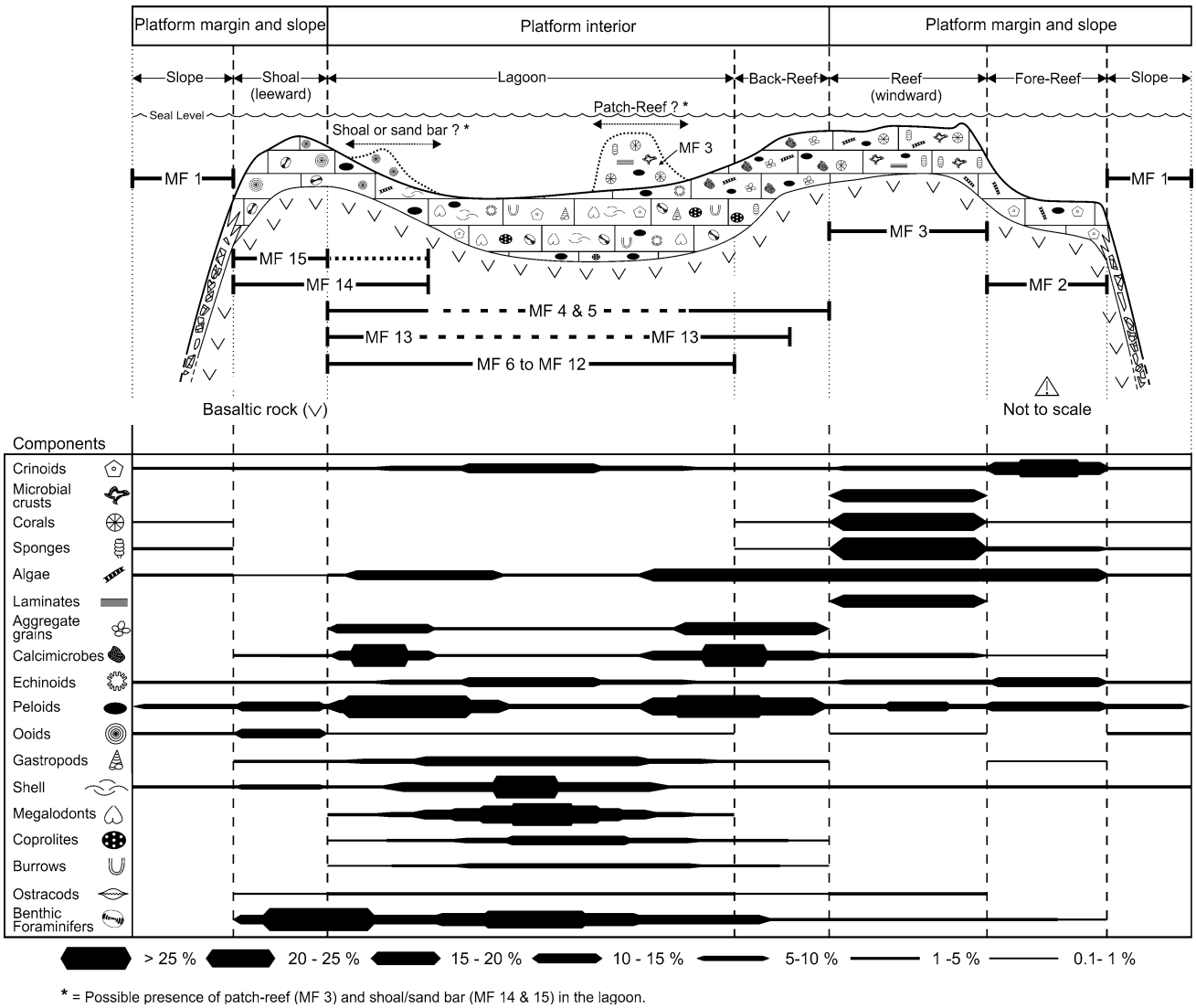

Fig. 12 Speculative depositional profile of a mid-oceanic atoll-top buildup carbonates illustrating one of the possible spatial distributions of the Upper Triassic microfacies recognized in the Sambosan AC in Kyushu Island. The distribution pattern of biotic components is also indicated as well as their relative abundance estimated for each microfacies using the comparison charts of Flügel (2004) and point-counting analysis

Speculative depositional profile

Although the distribution of outcrops studied is isolated and sections of sequences in stratigraphic order are rare, precluding accurate reconstruction of the original facies distribution, we tentatively present a speculative depositional profile on which the above-described and interpreted microfacies are replaced (Fig. 12). In addition, the distribution patterns of biotic components in reef, shoal, and lagoon facies are indicated as well as their relative abundance using the comparison charts of Flügel (2004) and point counting analysis.

The juxtaposition of facies on the suggested profile is based on lithologies, facies interpretation, and also on comparison to depositional settings of intact time-equivalent platforms such as Dachstein Platform (Flügel 1981), Dolomites (Blendinger and Blendinger 1989), Triassic limestones of Sikhote-Alin (Punina 1997), Triassic carbonates of United Arab Emirates and Oman (Bernecker 1996; Maurer et al. 2008), and modern isolated carbonate platforms such as Andros and other Islands of the Bahamas (Blatt et al. 1980; Hine et al. 1981), Kapingamarangi Atoll (Mckee et al. 1959), Marshall Islands (Enewetak and Bikini Atolls, Atkinson et al. (1981), the atoll system of the Maldives (Purdy and Bertram 1993) and the Banco Chinchorro (Gischler and Lomando 1999; Gischler and Möder 2009).

The Upper Triassic Sambosan limestones show characteristics of typical isolated shallow-water carbonate platforms or oceanic atolls formed on extinct and subsiding volcanoes. Commonly, raised reefal rims, steep outer

slopes and low coral islets encircling shallow to deep lagoons ranging from less than 1 km to more than 130 km in diameter characterize such oceanic atolls (Flügel 2004). The larger platforms may build sediment piles hundreds of meters thick. Generally, isolated or "unattached" carbonate platforms are morphologically variable. The margins of isolated platforms should be ramp-like, but more typically, are stepper than 15° (Wright and Burchette 1996). The platform margin may be rimmed either by reefs or by skeletal or oolitic sand shoals while the interior is generally mud-dominated and may have restricted circulation with the open ocean. The seamounts surrounded by deep water are strongly influenced by the orientation of dominant winds and waves. In this case, reefs develop preferentially along windward margins, where wave current activity is highest. All these general remarks are obvious in modern settings such as the Great Bahama Bank or modern oceanic atolls (Mckee et al. 1959; Atkinson et al. 1981; Hine et al. 1981; Guilcher 1988; Purdy and Bertram 1993), but they are more difficult to establish for ancient records such as seamounts of the Sambosan AC. Nevertheless, as in ancient and modern isolated platforms (Dolomites, Kapingamarangi Atoll, Marshall and Maldives Islands), our study shows a range of different environments and biofacies related to local variations in wave energy, temperature, salinity, nutrient supply, turbidity, and substrate across the platform.

Thus, our profile corresponds to a conceptual atoll-type platform illustrating the possible location of microfacies deposition and their spatial distribution patterns during a sea-level highstand situation. Neither scale nor precise timing are given in the profile since these indications remain uncertain. Nevertheless, according to the Sambosan AC distribution in the Kyushu Island, we suppose that the Upper Triassic isolated carbonate platform of this study might have an extension of around 100 km or more.

The spatial distribution of the recognized microfacies and the interpretation of their likely depositional settings allow the distinction of five main environments (Fig. 12): (1) shoal: MF 14 and MF 15, foraminiferal grainstone and oolitic-coated grains packstone-grainstone, respectively; (2) lagoon and back-reef: MF 4 to MF 13 with large, cm-scale, megalodont shells; (3) reef and/or patch-reef: MF 3 with microbial encrusters, stromatolites, spongiostromata crusts, spongiomorphids, algae, sponges, and corals; (4) fore-reef: MF 2, rich in crinoid fragments; and (5) slope: MF 1, limestone microbreccia here considered as records of gravitational deposits. These facies, grouped into the platform margin and slope and the platform interior, are discussed below. MF 16 and MF 17 are not represented in the profile because they correspond to basinal deposits.

Platform margin and slope

The platform margin and slope contains MF 1 to MF 3, MF 14 and MF 15 (Fig. 12). They correspond to slope deposits (MF 1), fore-reef or outer margin (MF 2), reef margin and/or patch-reef (MF 3) and to shoal–sand bar system (MF 14 and MF 15). We assume here that the slope of the platform and seamount should be uniformly steep, surrounding the entire platform, and that the margins of the hypothetic Sambosan isolated carbonate platform are either a skeletal or oolitic shoal rim, or a reef. However, this Late Triassic platform was not necessarily continuously rimmed as observed in the coeval isolated carbonate platforms of Dolomites, or in the Great Bahama Bank and numerous modern atolls (e.g., Enewetak Atoll, Atkinson et al. 1981 or Kapingamarangi Atoll, Mckee et al. 1959). Based on the components found in MF 14 and MF 15 (benthic foraminifers, gastropods, bivalves shells and micritized peloids, total absence of reef organisms), we suggest that the shoal should be located in the leeward margin (Blendinger and Blendinger 1989). Consequently, the reef and fore-reef might be located far from the shoal on the windward margin. Furthermore, the presence in the "external" lagoon of small shoals or sand bars, as well as patch-reefs, cannot be ruled out.

We believe that reefs or shoal are not continuous, asymmetric, and separated by channels that allow tidal exchange between platform and ocean, as in some modern shoals (e.g., Lily Bank on Little Bahama Bank, Hine 1977). This geometry may explain the sediment distribution and the water circulation (cementation) into the platform interior (Atkinson et al. 1981) and the presence of "open-marine" foraminifers such as nodosariids and duostominids within the lagoon. Atkinson et al. (1981) showed for the Enewetak Atoll (Marshall Islands) that windward and leeward cross-reef currents, channel currents, and tidal flow are the major factors influencing water and sediments exchanges between atoll lagoons and surrounding ocean. These factors depend of the local wave climate, tidal conditions, and atoll morphology.

The platform interior

The platform interior consists of ten microfacies: MF 4 to MF 13 (Fig. 12).

MF 4 to MF 13 have the largest spatial distribution in the profile and show characteristics of a lagoonal depositional setting. Field evidence and thin-sections clearly reveal the existence of two main lagoonal facies types: first, a low-energetic lagoonal mudstone to packstone with megalodontids, foraminifera, burrows and echinoderms (MF 6 to MF 13); second a high-energetic lagoonal

packstone-grainstone with aggregates, grapestones, coated grains, and porostomata (MF 4 to MF 5).

In the field, the facies distribution and their transitional contacts within the lagoon are rarely observed, except for the locality 17. In our speculative model, these microfacies could be located all over the lagoon with various possible lateral distributions depending on diverse factors such as sea level, energy, winds, salinity, temperature, nutrient supply, turbidity, and platform morphology. Yet, we postulate that MF 4 and MF 5, indicating intense water circulation, may possibly be located either in the back-reef or in the external lagoon close to the shoal and/or reefs. MF 6 and MF 7 (mudstone) should be placed in the lowest-energy, protected part of the platform interior, or close to the reefs, which may have acted as barrier for the wind-driven currents (Blatt et al. 1980; Halley et al. 1983). MF 8 and MF 10 are often reported as associated microfacies in various Triassic Tethyan platforms (Dachstein in Austria, Dolomites in Italy, platforms in the United Arab Emirates and Oman).

The presence in the lagoon of "open-marine" foraminifers including *Frondicularia* sp. (nodosariids) in MF 7 to 13 and *Duostomina* sp., *Variostoma* sp. and *Diplotremina* sp. especially in MF 4 and MF 5 supports the assumption that reefs and margins of the seamount were not continuous, but cut by channels that allow tidal exchange between the platform interior and the ocean (Atkinson et al. 1981). Water salinities in such settings may be predominantly normal marine to hypersaline.

Biostratigraphy

From a biostratigraphic point of view, data on MF 1 to MF 15 indicate an evolution of carbonate deposition from Late Carnian to Rhaetian. However, our speculative profile corresponds to the maximum growth of the atoll-type carbonates (highstand situation), on which all of the recognized microfacies are represented without time control. Nevertheless, the following scenario is proposed, based on the microfacies analysis, sedimentological, and biostratigraphic data.

As indicated by foraminiferal assemblages, we suggest that MF 7 (and locally MF 12) represent the initial Late Carnian stage of sedimentation in the lagoon. Almost at the same time, the first stage of reef growing is initiated. The ooid bank (MF 14 and MF 15) and the main lagoonal facies (MF 8 to MF 13) deposited principally during Norian in parallel with the reef growth. Recent results from Onoue and Stanley (2008) showed that reef continues to grow with inozoan sponges and coral on a bank margin during Norian and develops some *Retiophyllia* framebuilding during the Late Norian to Rhaetian time. No post-Triassic shallow-water limestones are documented in the Sambosan AC up to now. Apparently, shallow-water platform carbonate deposition stopped by that time, supposedly due to a sea-level rise and to giant submarine landslides of the seamount (Onoue and Stanley 2008).

Conclusions

The Upper Triassic limestones of the Sambosan AC (Kyushu Island, Japan) provides both valuable sedimentological data for the interpretation of the depositional environment and paleontological information useful for biostratigraphy, paleoecology, and paleogeography.

The Upper Triassic shallow-water limestone of the Sambosan AC represents deposits of an isolated carbonate platform that formed upon extinct and subsiding volcanoes.

Seamount eruption is Carnian in age based on conodonts originating from micritic interpillow limestones. The basaltic rocks show a typical OIB geochemical signature. The distribution patterns of the Sambosan AC throughout Japan points to an actual wide seamount province upon which Upper Triassic atoll-type carbonates developed.

Limestones crop out between chert, basaltic, and terrigenous units. Although sections preserved in their original stratigraphic order and with sedimentary structures are rare, the studied limestone rocks crop out as three modes of occurrence: massive limestone blocks (type 1), limestone breccia (type 2), and limestone pebbles (type 3).

Seventeen microfacies types have been defined with special focus on benthic foraminifers of shallow-water limestones. The microfacies interpretation of the Upper Triassic limestones and their comparison to ancient and modern depositional environments suggest a speculative depositional profile composed of shoal, lagoon, back-reef, reef, fore-reef and slope environments (MF 1 to MF 15). These facies are interpreted as atoll-type margin, slope, and platform interior deposits. The deeper basin located all around the seamount is composed of cherts and pelagic deeper-water limestone (MF 16 and MF 17).

Biostratigraphy based on foraminifers allows us to constrain the timing of the sedimentation of the Sambosan AC: the shallow-water limestones deposited from the Late Carnian to Rhaetian, with the main carbonate production during the Norian. More precisely, we postulate that during the Late Carnian a first stage of reef growth initiated. At the same time, a thin-bedded dark limestone (MF 7) and molluscan-burrowed wackestone (MF 12) was deposited in the platform interior, corresponding to the formation of the lagoon. We propose that the ooid bank or sand bar (MF 14 and MF 15) and the main lagoon (MF 8 to MF 13) formed principally during the Norian in parallel with the continuous growth of the reef. The deeper-water pelagic limestone,

intercalated between bedded cherts, has been deposited during Late Carnian to Early Norian time.

The foraminifers, bivalves, corals, and sponges show ubiquitous affinities to the tropical Tethyan fauna. Furthermore, Sambosan foraminifers exhibit strong similarities with those foraminiferal association from Oman and Indonesia islands (Sulawesi, Seram).

Thus, a paleoposition of the Sambosan large seamount province in low to middle tropical/subtropical latitudinal zone of the southern hemisphere, not so far from the paleomargin of Indonesia during the Late Triassic is likely.

Acknowledgments We wish to thank the Facies reviewers W. Piller and O. Weidlich for their very constructive criticisms in their review process of the first draft, as well as an anonymous reviewer. We thank the editor, A. Freiwald, for his advice and comments, which improved the manuscript. Finally, we also thank F. Kobayashi for sharing his samples containing the well-preserved index foraminifer *Triasina hantkeni*. Fieldwork was supported by the Swiss National Science Foundation (Grant # 200021-113816 to R. Martini).

References

Al-Shaibani SK, Carter DJ, Zaninetti L (1983) Geological and micropalaeontological investigations in the Upper Triassic (Asinepe Limestone) of Seram, outer Banda Arc, Indonesia. Arch Sci 36:297–313

Alve E (1999) Colonization of new habitats by benthic foraminifera: a review. Earth-Sci Rev 46:167–185

Alve E, Goldstein ST (2003) Propagule transport as a key method of dispersal in benthic foraminifera (Protista). Limnol Oceanogr 48:2163–2170

Atkinson M, Smith SV, Stroup ED (1981) Circulation in Enewetak Atoll lagoon. Limnol Oceanogr 26:1074–1083

Beatty TW, Zonneveld JP, Henderson CH (2008) Anomalously diverse early Triassic ichnofossil assemblages in northwest Pangea: a case for a shallow-marine habitable zone. Geol Soc Am 36:771–774

Becker MJ, Dodd JR (1994) Depositional history of a Mississippian crinoidal mound on the east flank of the Illinois Basin. Carbonate Evaporite 9:76–88

Bernecker M (1996) Upper Triassic reefs of the Oman Mountains: data from the South Tethyan margin. Facies 34:41–76

Bernecker M (2005) Late Triassic reefs from the Northwest and South Tethys: distribution, setting, and biotic composition. Facies 51:442–453

Bernecker M, Weidlich O, Flügel E (1999) Response of Triassic reef coral communities to sea-level fluctuations, storms and sedimentation. Evidence from a spectacular outcrop (Adnet, Austria). Facies 40:229–280

Blatt H, Middleton GV, Murray RC (1980) Origin of sedimentary rocks. Prentice-Hall, Englewood Cliffs, NJ, 634 pp

Blendinger W, Blendinger E (1989) Windward-leeward effects on Triassic carbonate bank margin facies of the Dolomites, northern Italy. Sedim Geol 64:143–166

Bosellini A, Masetti D, Sarti M (1981) A Jurassic 'Tongue of the Ocean' infilled with oolitic sands: the Belluno Trough, Venetian Alps, Italy. Mar Geol 44:59–95

Bralower TJ, Brown PR, Siesser WG (1991) Significance of Upper Triassic nannofossils from the southern hemisphere (ODP Leg 122, Wombat Plateau, NW Australia). Mar Micropaleontol 17:119–154

Carcione L, Martini R, Zaninetti L (2003) The Lercara Formation (Upper Permian ?—Lower to Middle Triassic, Sicily): a syn-rift deposit? Abstract of the 11th Meeting of Swiss Sedimentologists, Fribourg, pp 26–27

Chablais J, Martini R, Samankassou E, Onoue T, Sano H (2007) Upper Triassic foraminifers from the mid-oceanic atoll-type carbonate of the Sambosan Accretionary Complex (Kyushu and Shikoku Islands, Japan). Abstracts 5th Swiss Geoscience Meeting, Geneva, pp 193–194

Chablais J, Martini R, Rigaud S, Samankassou E, Onoue T, Sano H (2008) New Upper Triassic foraminifers of Sambosan Accretionary Complex (Japan): a tool for sedimentological and paleobiogeographic understanding of the Panthalassan Ocean. Abstracts 33rd International Geological Congress, Oslo, HPF-12, Environmental micropaleontology: Past, Present, Future—Part 2

Dunham RJ (1962) Classification of carbonate rocks according to depositional texture. In: Ham WE (ed) Classification of carbonate rocks, AAPG Mem 1:108–121

Enos P, Samankassou E (1998) Lofer cyclothems revisited (Late Triassic, Northern Alps, Austria). Facies 38:207–228

Faure M, Natal'in B (1992) The geodynamic evolution of the eastern Eurasian margin in Mesozoic times. Tectonophysics 208:397–411

Fischer AG (1964) The Lofer cyclothems of the Alpine Triassic. In: Meeriam DF (ed) Symposium on cyclic sedimentation. Kansas Geol Soc Bull 169:107–149

Flügel E (1981) Paleoecology and facies of Upper Triassic reefs in the Northern Calcareous Alps. SEPM Spec Publ 30:291–359

Flügel E (1982) Evolution of Triassic reefs: current concepts and problems. Facies 6:297–328

Flügel E (2002) Triassic reef patterns. In: Kiessling W, Flügel E, Golonka J (eds) Phanerozoic reef patterns. SEPM Spec Publ 72:391–464

Flügel E (2004) Microfacies of carbonate rocks. Springer, Berlin Heidelberg New York, 976 pp

Flügel E, Stanley GD (1984) Reorganisation, development and evolution of post-Permian reefs and reef organisms. Paleontographica Am 54:177–186

Fujita H (1989) Stratigraphy and geologic structure of the pre-Neogene strata in the Central Ryukyu Islands. J Sci Hiroshima Univ Ser C Geol Min 9:237–283

Gazdzicki A (1983) Foraminifers and biostratigraphy of Upper Triassic and Lower Jurassic of the Slovakian and Polish Carpathians. Paleontol Pol 44:109–169

Gischler E, Lomando AJ (1999) Recent sedimentary facies of isolated carbonate platforms, Belize, Yucatan system, Central America. J Sediment Res 69:747–763

Gischler E, Möder A (2009) Modern benthic foraminifera on Banco Chinchorro, Quintana Roo, Mexico. Facies 55:27–35

Guilcher A (1988) Coral reef geomorphology. Wiley, Chichester, 248 pp

Halley RB, Harris PM, Hine AC (1983) Bank margin environment. In: Scholle PA, Bebout DG, Moore CH (eds) Carbonate depositional environments. AAPG Mem 33:463–506

Hine AC (1977) Lily Bank, Bahamas: history of an active oolite sand shoal. J Sedim Petrol 47:1554–1581

Hine AC, Wilber RJ, Neumann AC (1981) Carbonate sand bodies along contrasting shallow-bank margins facing open seaways, northern Bahamas. AAPG Bull 65:261–290

Hohenegger J, Piller W (1975) Ökologie und systematische Stellung der Foraminiferen im gebankten Dachsteinkalk (Obertrias) des nördlichen Toten Gebirges (Oberösterreich). Palaeogeogr Palaeoclim Palaeoecol 18:241–276

Hudson JD (1982) Pyrite in ammonite-bearing shales from the Jurassic of England and Germany. Sedimentology 29:639–667
Ichikawa K (1990) Pre-Cretaceous terranes of Japan. Publ IGCP Proj 224:1–12
Isozaki Y (1997) Jurassic accretion tectonics of Japan. Island Arc 6:25–51
Jafer SA (1983) Significance of Late Triassic calcareous nannoplankton from Austria and southern Germany. Neues Jahrb Geol Paläontol Abh 166:218–259
Kanmera K (1964) Triassic coral faunas from the Konosé Group in Kyushu. Mem Fac Sci Kyushu Univ Ser D 15:117–147
Kanmera K (1969) Litho-and bio-facies of Permo-Triassic geosynclinal limestone of the Sambosan Belt in southern Kyushu. Spec Publ Palaeontol Soc Jpn 14:13–39
Kanmera K, Furukawa H (1964) Stratigraphy of the Upper Permian and Triassic Konose Group of the Sambosan belt in Kyushu. Sci Rep Fac Sci Kyushu Univ Geol 6:237–258
Kiessling W, Flügel E (2000) Late Paleozoic and Late Triassic limestones from North Palawan Block (Philippines): microfacies and paleogeographical implications. Facies 43:39–78
Kiessling W, Flügel E, Golonka J (1999) Paleoreef maps: evaluation of a comprehensive database on Phanerozoic reefs. AAPG Bull 83:1552–1587
Kobayashi T (1931) Notes on a new occurrence of Ladino-Carnic limestone at Sambosan, Tosa Province, Japan. Jpn J Geol Geogr 8:251–258
Kobayashi F (2003) Paleogeographic constraints on the tectonic evolution of the Maizuru Terrane of southwest Japan to the eastern continental margin of South China during the Permian and Triassic. Palaeogeogr Palaeoclim Palaeoecol 195:299–317
Koike T (1981) Biostratigraphy of Triassic conodonts in Japan. Science reports of the Yokohama National University. Sect II. Biol Geol Sci 28:25–46
Kojima S (1989) Mesozoic terrane accretion in northeast China, Sikhote-Alin and Japan regions. Palaeogeogr Palaeoclim Palaeoecol 69:213–232
Kristan-Tollmann E (1986) Triassic of the Tethys and its relations with the Triassic of the Pacific Realm. Int Symp Shallow Tethys 2:169–186
Kristan-Tollmann E (1988) A comparison of Late Triassic agglutinated foraminifera of western and eastern Tethys. Abh Geol B A 41:245–253
Kristan-Tollmann E (1991) Triassic Tethyan microfauna in Dachstein limestone blocks in Japan. In: Kotaka T, Dickins JM, McKenzie KG, Mori K, Ogasawara K, Stanley GD Jr (eds) Shallow Tethys 3, Proceedings of the Int Symp on Shallow Tethys, Sendai, 1990. Saito Ho-on Kai Spec Publ 3, Saito Ho-on Kai, Sendai, Japan, pp 35–49
Kristan-Tollmann E and Gramann F (1992) Paleontological Evidence for the Triassic Age of Rocks Dredged from the Northern Exmouth Plateau (Tethyan Foraminifers, Echinoderms, and Ostracodes). In: Rad U von, Haq BU, O'Connell, De Carlo EH (eds) Proc Ocean Drill Program, Sci Result 122:463–474
Martini R, Vachard D, Zaninetti L, Cirilli S, Cornée JJ, Lathuilière B, Villeneuve M (1997) Sedimentology, stratigraphy and micropaleontology of the Upper Triassic reefal series in Eastern Sulawesi (Indonesia). Palaeogeogr Palaeoclim Palaeoecol 128:157–174
Martini R, Zaninetti L, Lathuilière B, Cirilli S, Cornée JJ, Villeneuve M (2004) Upper Triassic Carbonate deposits of Seram (Indonesia): palaeogeographic and geodynamic implications. Palaeogeogr Palaeoclim Palaeoecol 206:75–102
Matsuoka A (1992) Jurassic-Early Cretaceous tectonic evolution of the Southern Chichibu terrane, southwest Japan. Palaeogeogr Palaeoclim Palaeoecol 96:71–88
Matsuoka A, Yao A (1990) Southern Chichibu Terrane. Pre-Cretaceous terranes of Japan. Publ IGCP Proj 224:203–216
Maurer F, Rettori R, Martini R (2008) Triassic stratigraphy and evolution of the Arabian shelf in the northern United Arab Emirates. Int J Earth Sci 97:765–784
Mckee ED, Chronic J, Leopold EB (1959) Sedimentary belts in lagoon of Kapingamarangi atoll. AAPG Bull 43:501–562
Michalik J (1982) Uppermost Triassic short-lived bioherm complexes in the fatric, western Carpathians. Facies 6:129–145
Michalik J, Rehakova D, Zirt J (1993) Upper Jurassic and Lower Cretaceous facies, microplankton and crinoids in the Kuchyna Unit, Male Karpaty Mts. Geol Carpathica 44:161–176
Miconnet P, Ciarapica G, Zaninetti L (1983) Faune à Foraminifères du Trias supérieur d'affinité sud-téthysienne dans l'Apennin méridional (Bassin de Lagonegro, province de Potenza, Italie); comparaison avec l'Apennin septentrional. Rev Paléobiol 2:131–147
Mullins HT, Cook HE (1986) Carbonate apron models: alternatives to the submarine fan model for paleoenvironmental analysis and hydrocarbon exploration. Sediment Geol 48:37–79
Nishizono Y (1996) Mesozoic convergent process of the Southern Chichibu Terrane in West Kyushu, Japan, on the basis of Triassic to Early Cretaceous radiolarian biostratigraphy. Kumamoto J Sci Earth Sci 14:45–226
Ogawa Y, Taniguchi H (1989) Origin and emplacement process of the basaltic rocks in the accretionary complexes and structural belts in Japan in view of minor element analysis and mode of occurrence. J Geogr 98:118–132
Onoue T, Sano H (2007) Triassic mid-oceanic sedimentation in Panthalassa Ocean: Sambosan Accretionary Complex, Japan. Island Arc 16:173–190
Onoue T, Stanley GD (2008) Sedimentary facies from Upper Triassic reefal limestone of the Sambosan Accretionary Complex in Japan: mid-ocean patch reef development in the Panthalassa Ocean. Facies 54:529–547
Onoue T, Tanaka H (2002) Discovery of Upper Triassic bivalves from Sambosan Subterrane, Itsuki area, Kumamoto Prefecture, and its geologic implication. J Geol Soc Jpn 108:610–613
Onoue T, Tanaka H (2005) Late Triassic bivalves from Sambosan Accretionary Complex, southwest Japan, and their biogeographic implications. Paleontol Res 9:15–25
Onoue T, Nagai K, Kamishima A, Seno M, Sano H (2004) Origin of basalts from Sambosan Accretionary Complex, Shikoku and Kyushu. J Geol Soc Jpn 110:222–236
Onoue T, Chablais J, Martini R (2009) Upper Triassic reefal limestone from the Sambosan Accretionary Complex in Japan and its geological implication. J Geol Soc Jpn 115:292–295
Pawlowski J, Holzmann M (2008) Diversity and geographic distribution of benthic foraminifera: a molecular perspective. Biodivers Conserv 17:317–328
Piller W (1978) Involutinacea (Foraminifera) der Trias und des Lias. Beitr Paläont Österreich 5:1–164
Punina TA (1997) Classification and correlation of Triassic limestones in Sikhote-Alin on the basis of corals. In: Dickins JM, Yan Z, Yin H, Lucas SG, Acharya SK (eds) Late Paleozoic and Early Mesozoic Circum-Pacific event and their global correlation. Cambridge University Press, Cambridge, pp 186–192
Purdy EG, Bertram GT (1993) Carbonate concepts from the Maldives, Indian Ocean. Am Assoc Pet Geol Studies Geol 34:1–56
Rai J, Upadhyay R, Sinha AH (2004) First Late Triassic nannofossil record from the Neo-Tethyan sediments of the Indus-Tsangpo Sututre Zone, Ladakh Himalaya, India. Curr Sci 86:774–777
Reid RP (1987) Nonskeletal peloidal precipitates in Upper Triassic reefs, Yukon Territory (Canada). J Sediment Petrol 57:893–900

Schäfer P, Senowbari-Daryan B (1981) Facies development and paleoecologic zonation of four Upper Triassic patch-reefs, Northern Calcareous Alps near Salzburg, Austria. In: Toomey DF (ed) European fossil reef models. SEPM Spec Publ 30:241–259

Schäfer P, Senowbari-Daryan B (1982) The Upper Triassic Pantokrator Limestone of Hydra (Greece): an example of a prograding reef complex. Facies 6:147–163

Senowbari-Daryan B, Maurer F (2008) Upper Triassic (Norian) hypercalcified sponges from the Musandam Peninsula (United Arab Emirates). Facies 54:433–460

Senowbari-Daryan B, Ciarapica G, Cirilli S, Zaninetti L (1985) Nouvelles observations d'*Altinerina meridionalis* Zaninetti, Ciarapica, Decrouez et Miconnet, 1984 (Foraminifères) dans le Trias supérieur (Norien récifal de la Plate-forme panormide, Sicile. Rev Paléobiol 4:301–306

Senowbari-Daryan B, Bernecker M, Krystyn L, Siblik M (1999) Carnian reef biota from a megabreccia of the Hawasina complex (Al Aquil, Oman). Riv Ital Paleont Stratigr 105:327–342

Senowbari-Daryan B, Chablais J, Martini R (2009) New crustacean microcoprolites of the Upper Triassic limestones of the Sambosan Accretionary Complex, Japan. J Paleont (in press)

Stanley GD (1994) Late Paleozoic and early Mesozoic reef-building organisms and paleogeography: the Tethyan-North American connection. Cour Forsch Inst Senkenberg 172:69–75

Stanley GD, Gonzalez-Leon CM (1997) New Late Triassic scleractinian corals from the Antimonio Formation, northwestern Sonora, Mexico. Rev Mex Cie Geol 14:202–207

Taira A, Tokuyama H, Soh W (1989) Accretion tectonics and evolution of Japan. In: Avraham Ben (ed) The evolution of the Pacific Ocean Margins. Oxford University Press, Oxford, pp 100–123

Takami M, Takemura R, Nishimura Y, Kojima T (1999) Reconstruction of oceanic plate stratigraphies and unit division of Jurassic-Early Cretaceous accretionary complexes in the Okinawa Islands, central Ryukyu Island Arc. J Geol Soc Jpn 105:866–880

Tamura M (1972) Myophorian fossils discovered from the Konose Group, Kumamoto Prefecture, Japan, with a note on Japanese myophoriids. Mem Fac Educ Kumamoto Univ Nat Sci 21:66–73

Tamura M (1981) Preliminary report on the Upper Triassic megalodonts discovered in South Kyushu, Japan. Proc Jpn Acad 57:290–295

Tamura M (1983) Megalodonts and megalodont limestone in Japan [J]. Mem Fac Educ Kumamoto Univ Nat Sci 32:7–28

Tichy G (1975) Fossilfunde aus dem Hauptdolomit (Nor, Trias) der östlichen Gailtaler Alpen (Kärnten, Österreich). Ann Nathist Mus Wien 79:57–100

Villeneuve M, Cornée JJ, Martini R, Zaninetti L, Rehault JP, Burhanudin S, Malod J (1994) Upper Triassic shallow water limestones in the Sinta Ridge (Banda Sea- Indonesia). Geo-Mar Lett 14:29–35

Wakita K, Metcalfe I (2005) Ocean plate stratigraphy in East and Southeast Asia. J Asian Earth Sci 24:679–702

Weidlich O, Bernecker M, Flügel E (1993) Combined quantitative analysis and microfacies studies of ancient reefs: an integrated approach to Upper Permian and Upper Triassic reef carbonates (Sultanate of Oman). Facies 28:115–144

Wright VP, Burchette (1996) Shallow-water carbonate environments. In: Reading HG (ed) Sedimentary environments: processes, facies and stratigraphy. Blackwell Science, Oxford, pp 325–394

Yao A (1990) Triassic and Jurassic radiolarians. In: Ichikawa K, Mizutani S, Hara I, Hada S, Yao A (eds) Pre-Cretaceous terrane of Japan. IGCP, Osaka City University, pp 329–345

Zaninetti L (1976) Les Foraminifères du Trias-Essai de synthèse et corrélation entre les domaines mésogéen européen et asiatique. Riv Ital Paleontol Stratigr 82:1–258

Zaninetti L, Ciarapica G, Decrouez D, Miconnet P (1984) *Altinerina meridionalis* n.gen., n.sp., un foraminifère du Trias supérieur (Norien) récifal de l'Apennin méridonal et de la Sicile, Italie. Rev Paléobiol 3:15–18

Zaninetti L, Martini R, Dumont T (1992) Triassic foraminifera from sites 761 and 764, Wombat Plateau, northwestern Australia. In: von Rad U, Haq BU, O'Connell, De Carlo EH (eds) Proc Ocean Drill Program, Sci Res 122:427–436